

1 **Analogue experiments on releasing and restraining bends and their**
2 **application to the study of the Barents Shear Margin**

3
4
5
6 **Roy H. Gabrielsen ¹⁾, Panagiotis A. Giannenas³⁾, Dimitrios Sokoutis^{1,3)}, Ernst**
7 **Willingshofer³⁾, Muhammad Hassaan^{1,4)} & Jan Inge Faleide¹⁾**

8
9 ¹⁾Department of Geosciences, University of Oslo, Norway

10 ²⁾panagiotis-athanasios.giannenos@univ-rennes1.fr

11 ³⁾ Faculty of Geosciences, Utrecht University, the Netherlands

12 ⁴⁾ Vår Energi AS, Grundingen 3, 0250 Oslo, Norway

13
14
15 **Corresponding author: Roy H. Gabrielsen (r.h.gabrielsen@geo.uio.no)**

16
17 **ORCI-id:**

18 Jan Inge Faleide: 0000-0001-8032-2015

19 Roy H. Gabrielsen: 0000-0001-5427-8404

20 Muhammad Hassaan: 0000-0001-6004-8557

21
22
23
24
25 **Abstract:**

26 The Barents Shear Margin separates the Svalbard and Barents Sea from the North
27 Atlantic. During the break-up of the North Atlantic the plate tectonic configuration
28 was characterized by sequential dextral shear, extension, and finally contraction
29 and inversion. This generated a complex zone of deformation that contains several
30 structural families of over-lapping and reactivated structures.

31 A series of crustal-scale analogue experiments, utilizing a scaled stratified sand-
32 silicon polymer sequence were utilized in the study of the structural evolution of
33 the shear margin.

34
35 The most significant observations of particular significance for
36 ~~interpreting~~ interpreting the structural configuration of the Barents Shear
37 Margin are:

38 1) Prominent early-stage positive structural elements (e.g. folds, push-ups)
39 interacted with younger (e.g. inversion) structures and contributed to a hybrid
40 final structural pattern.

41 2) Several ~~of the~~ structural features that were initiated during the early (dextral
42 shear) stage became overprinted and obliterated in the subsequent stages.

43 3) All master faults, pull-part basins and extensional shear duplexes initiated
44 during the shear stage quickly became linked in the extension stage, generating a
45 connected basin system along the entire shear margin at the stage of maximum
46 extension.

47 4) The fold pattern generated during the terminal stage (contraction/inversion
48 became dominant in the basin areas and was characterized by fold axes ~~with~~
49 ~~traces~~ striking parallel to the basin margins. These folds, however, ~~most~~ strongly
50 affected the shallow intra-basin layers.

51 The experiments reproduced the geometry and positions of the major basins and
52 relations between structural elements (fault and fold systems) as observed along
53 and adjacent to the Barents Shear Margin. This supports the present structural
54 model for the shear margin.

55
56

57 **Plain language summary:**

58 The Barents Shear Margin defines the border between the relatively shallow
59 Barents Sea that is situated on a continental plate, and the deep ocean. The margin
60 is characterized by a complex structural pattern that has resulted from the
61 opening and separation of the continent and the ocean, starting c. 65 million years
62 ago. This history included on phase of right-lateral shear and one phase of
63 spreading, the latter including a subphase of shortening, perhaps due to plate
64 tectonic reorganizations. The area has been mapped by the study of reflection
65 seismic lines for decades, but many details of its development is not yet fully
66 constrained. We therefore ran a set of scaled experiments to investigate what kind
67 of structures could be expected in this kind of tectonic environment, and to figure
68 out what is a reasonable time relation between them. From these experiments we
69 deduced several types of structures/faults, folds and sedimentary basins) that
70 helps us to improve the understanding of the history of the opening of the North
71 Atlantic.

72
73
74

75 **Key words:** Analogue experiments, dextral strike-slip, releasing and restraining
76 bends, multiple folding, Barents Shear Margin, basin inversion

77
78

79 **Introduction**

80
81 Physiography, width and structural style of the Norwegian continental margin
82 vary considerably along its strike (e.g. Faleide et al., 2008, 2015). The margin
83 includes a southern rifted segment between 60° and 70°N and a northern sheared-
84 rifted segment between 70° and 82°N (**Figure 1A**). The latter coincides with the
85 ocean-ward border of the western Barents Sea and Svalbard margins (e.g. Faleide
86 et al., 2008) and is referred to here as “the Barents Shear Margin”. This segment
87 coincides with the continent-ocean transition (COT) of the northernmost part of
88 the North Atlantic Ocean, and its configuration is typical for that of transform
89 margins where the structural pattern became established in an early stage of
90 shear, later to develop into an active continent-ocean passive margin (Masclé &
91 Blarez, 1987; Lorenzo, 1997; Seiler et al., 2010; Basile, 2015; Nemcok et al., 2016).
92 Late Cretaceous - Palaeocene shear, rifting, breakup and incipient spreading in the
93 North Atlantic was associated with voluminous magmatic activity, resulting in the
94 development of the North Atlantic Volcanic Province (Saunders et al., 1997;
95 Ganerød et al., 2010; Horni, 2017). According to its tectonic development, the
96 Barents Shear Margin (**Figure 1B**) incorporates, or is bordered by, several distinct
97 structural elements, some of which are associated with volcanism and halokinesis.
98 The multistage development combined with a complex geometry caused
99 interference between structures (and sediment systems) in different stages of the
100 margin development. Such relations are not always obvious, but interpretation
101 can be supported by the help of scale-models. ~~Combining~~ Combining the interpretation of
102 reflection seismic data and analogue modeling, therefore, we investigate
103 structures generated in (initial) dextral shear, the development into seafloor
104 spreading and subsequent contraction in this process, the later stages
105 [\(contraction\)](#) of which were likely influenced by plate reorganization (Talwani &
106 Eldholm, 1977, Gaina et al. 2009, see also see also Vågnes et al. 1998; Pascal &
107 Gabrielsen 2001; Pascal et al., 2005; Gac et al., 2016) or other far-field stresses
108 (Doré & Lundin, 1996; Lundin & Doré, 1997; Doré et al., 1999; 2016; Lundin et al.,
109 2013). The present experiments were designed to illuminate the structural
110 complexity affiliated with multistage sheared passive margins, so that the
111 significance of structural elements like fault and fold systems observed along the
112 Barents Shear Margin could be set into a dynamic context. The study area suffered

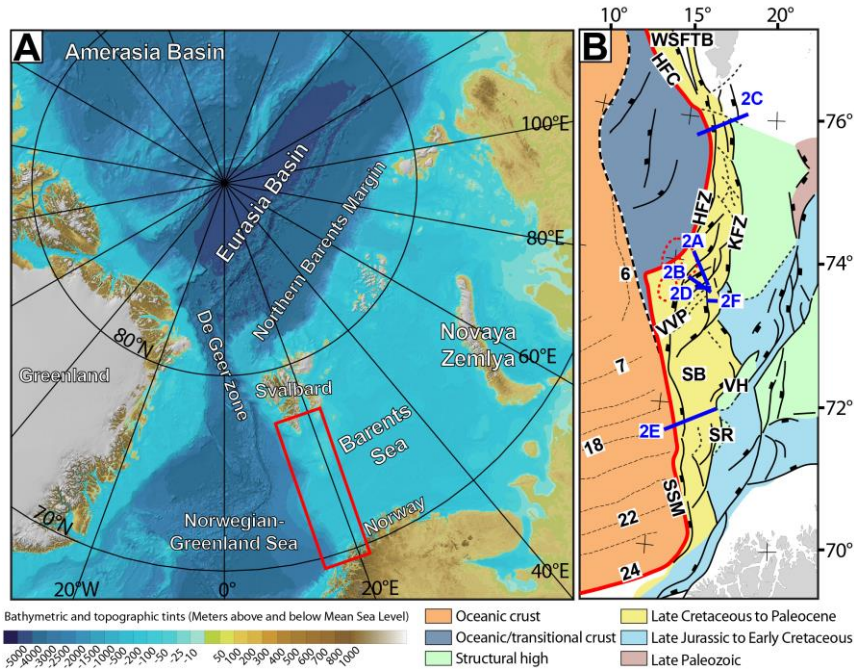


Figure 1: A) The Barents Sea provides is separated from the Norwegian-Greenland Sea by the de Geer transfer margin. Red box shows the present study area. **B)** Structural map Barents Sea shear margin. Note segmentation of the continent-ocean transition. Abbreviations (from north to south): WSFTB = West Spitsbergen Fold-and-Thrust Belt HFZ=Hornsund Fault Complex, KFC = Knølegga Fault Zone, VVP = Vestbakken Volcanic Province, SB = Sørvestsnaget Basin, VH=Veslemøy High, SR = Senja Ridge, SSM = Senja Shear Margin. Blue lines indicate position of seismic profiles in Figure 2 and red line X-X' shows western border of thinned crust (see also Figure 3). Chron numbers are indicated on oceanic crust area.

repeated and contrasting stages of deformation, including dextral shear, oblique extension, inversion and volcanic activity. This is a particular challenge in such tectonic settings, that are characterized by repeated overprinting and canabalization of ~~incipient by~~ younger structural elements. The experimental approach opens for the identification and characterization of the different stages of deformation and their affiliated structural elements ~~preceeding on the way to~~ the present-day margin geometry.

Regional background

134 In the following sections we provide definitions and a short description of the
135 ~~mainmost important~~ structural elements constituting the study area. The
136 structural elements are presented in-sequence from north to south and (**Figure**
137 **1B**).

138

139 The greater **Barents Shear Margin** is a part of the ~~preceeding and~~ more extensive
140 “De Geer Zone megashear system which linked the Norwegian Greenland Sea and
141 the Arctic Eurasia system (Eldholm et al., 1987; 2002; Faleide et al., 1988; Breivik
142 et al., 1998; 2003). Together with its conjugate Greenland counterpart it carries
143 the evidence of ~~an extensive period of structural development, starting with~~ post-
144 Caledonian (~~Devonian~~) extension ~~that and~~ culminating with Cenozoic break-up
145 of the North Atlantic (e.g. Brekke, 2000; Gabrielsen et al., 1990; Faleide et al., 1993;
146 Gudlaugsson et al., 1998). Two shear margin segments ~~that~~ are separated by a
147 central rift-dominated segment ~~can be identified along in~~ the Barents Shear Margin
148 (Myhre et al., 1982; Vågnes, 1997; Myhre & Eldholm, 1988; Ryseth et al., 2003;
149 Faleide et al., 1988; 1993; 2008). Each segment maintained ~~a particular signature~~
150 ~~concerning~~ the structural and magmatic characteristics of the crust during its
151 development. Of these the Senja Shear Margin is the southernmost segment,
152 originally termed the Senja Fracture Zone by Eldholm et al., (1987). Here, NNW-
153 SSE-striking folds interfere ~~with folds~~ with NE-SW-striking ~~structures axes~~
154 (Giennenas, 2018). Strain partitioning ~~characterizes the of may also have affected~~
155 ~~some of the other the~~ shear zone ~~system segments of the study area (e.g. Vest~~
156 ~~Spitsbergen; Leever et al. 2011a,b and the~~ Sørvestsnaget Basin; Kristensen et al.,
157 2017).

158

159 **The Hornsund Fault Zone and West Spitsbergen Fold-and Thrust Belt** form
160 the northernmost segment of the Barents Shear Margin and coincide with the
161 ~~southern northern~~ continuation of the De Geer Zone and the Senja Shear Margin.
162 The presently distinguishable master fault of this system is the Hornsund Fault
163 Zone, which together with the West Spitsbergen fold-and-thrust-belt provides a
164 type setting for transpression and strain partitioning (Harland, 1965; 1969; 1971;
165 Lowell, 1972; Gabrielsen et al., 1992; Maher et al., 1997; Leever et al., 2011 a,b).
166 Plate tectonic reconstructions suggest that the plate boundary accommodated c.

167 750 km along-strike [dextral](#) displacement and 20-40 km of shortening in the
168 Eocene (Bergh et al., 1997; Gaina et al., 2009).

169

170 **The Knølegga Fault Zone** can be seen as a part of the Hornsund fault system
171 extending from the southern tip of Spitsbergen (Gabrielsen et al., 1990). It trends
172 NNE-SSW to N-S and defines the western margin of the Stappen High. The vertical
173 displacement approaches 6 km. Although the main movements along the fault may
174 be Tertiary of age, it is likely that it was initiated much earlier. The Tertiary
175 displacement may have ~~had~~ a lateral (dextral) component (Gabrielsen et al.,
176 1990).

177

178 **The Vestbakken Volcanic Province** is the ~~main~~[central](#) topic of ~~this~~[the present](#)
179 contribution. It represents the [central](#) rifted segment of the Senja Shear Margin
180 and links the sheared margin segments ~~that are situated~~ to the north and south ~~of~~
181 ~~it and~~ occupying a ~~typical~~ right-double stepping (eastward) releasing-bend-
182 setting. Prominent volcanoes and sill-intrusions ~~suggest~~[display significant](#)
183 ~~magmatic activity, and~~ three distinct volcanic events ~~are distinguished~~ in the
184 Vestbakken Volcanic Province (Jebsen & Faleide, 1998; Faleide et al., 2008; Libak
185 et al., 2012). ~~The area has been affected by complex tectonics and both extensional~~
186 ~~and contractional structures are observed. It~~The Vestbakken Volcanic Province is
187 constrained to its east by the eastern boundary fault (EBF in **Figure 1B**), that is a
188 part of the Knølegga Fault Complex, separating the Vestbakken Volcanic Province
189 from the marginal Stappen High further to the east. To the south and southeast
190 the Vestbakken Volcanic Province drops gradually ~~towards~~[into](#) the Sørvestsnaget
191 Basin across the southern extension of the eastern boundary fault and its
192 associated faults. To the west and north the area is delineated by the continent –
193 ocean boundary/transition. The Vestbakken Volcanic Province includes both
194 extensional and contractional structures (eg. Jebsen & Faleide, 1998; Faleide et al.,
195 2008; Blaich et al., 2017). All other faults in this map are secondary faults, mainly
196 acting as accommodation structures to the master faults. Starting from the
197 southern part of the area and south of the well site, a population of secondary
198 faults is expressed as anastomosing faults traces.

199 ~~The Vestbakken Volcanic Province is delineated towards the east by an~~
200 ~~extensional top-west fault zone that parallels the Knølegga Fault Complex). The~~
201 ~~interior of the Vestbakken Volcanic Province is dominated by NE-SW striking~~
202 ~~extensional faults and associated fault blocks. Positive structural elements include~~
203 ~~inverted fault blocks, and wide-angle ($\lambda > 20$ km) anticlines (roll-over anticlines?)~~
204 ~~and domes that are overprinted by faults and folds with amplitudes and~~
205 ~~wavelengths on the hundred- and km-scales.~~

206 ~~The eastern boundary fault (EBF) is a top-west normal fault with a regional NNE-SSW~~
207 ~~strike, consisting of two separate, linked segments. Its northern segment dips more~~
208 ~~steeply to the WNW than the southern segment. The total vertical displacement as~~
209 ~~measured on the early Eocene level is in the order of 300 msec (450m), and the upper~~
210 ~~part of the hanging wall displays a normal drag modified by hanging wall tight antiline~~
211 ~~suggesting post early Miocene inversion. Several normal, dominantly NE-SW striking~~
212 ~~NW-facing normal faults transect the hanging wall of the EBF fault. The Central Fault~~
213 ~~(CF) is the largest of those and is hard linked to the central segment of the EBF fault is~~
214 ~~the largest of those. The Central Fault is the most prominent fault of a NW-SE striking~~
215 ~~fault population that characterizes the entire Vestbakken Volcanic Province. Two~~
216 ~~main~~ree~~ episodes of Cenozoic extensional faulting were identified in the~~
217 ~~Vestbakken Volcanic Province: (i) a late Paleocene-early Eocene event, which~~
218 ~~correlates in time with the continental break-up in the Norwegian-Greenland Sea,~~
219 ~~(ii) an early Oligocene event that is tentatively correlated to plate reorganization~~
220 ~~around 34 Ma activated mainly-NE-SW striking faults, and (iii) an extensional~~
221 ~~Pliocene event. Evidence of volcanic activity coincides with the first two of these~~
222 ~~events.~~

223 ~~The Vestbakken Volcanic Province is constrained to its east by the eastern~~
224 ~~boundary fault (EBF in Figure 1B), that is a part of the Knølegga Fault Complex,~~
225 ~~separating the Vestbakken Volcanic Province from the marginal Stappen High~~
226 ~~further to the east. To the south and southeast the Vestbakken Volcanic Province~~
227 ~~drops gradually into the Sørvestnaget Basin across the southern extension of the~~
228 ~~eastern boundary fault and its associated faults. To the west and north the area is~~
229 ~~delineated by the continent-ocean boundary/transition. The Vestbakken~~
230 ~~Volcanic Province includes both extensional and contractional structures (eg.~~
231 ~~Jebben & Faleide, 1998; Faleide et al., 2008; Blaich et al., 2017). All other faults in~~

232 ~~this map are secondary faults, mainly acting as accommodation structures to the~~
233 ~~master faults. Starting from the southern part of the area and south of the well site,~~
234 ~~a population of secondary faults is expressed as anastomosing faults traces.~~

235

236 **The Sørvestsnaget Basin** occupies the area east the COT between 71 and 73°N
237 and is characterized by an exceptionally thick Cretaceous-Cenozoic sequence
238 (Gabrielsen et al., 1990). To the west it is delineated by the Senja Shear Margin
239 and to the northeast it is separated from the Bjørnøya Basin by the southern part
240 of the Knølegga Fault Complex (Faleide et al., 1988). The position of the Senja
241 Ridge coincides with southeastern border of the Sørvestsnaget Basin (Figure 1B),
242 whereas the Vestbakken Volcanic Province is situated to its north. An episode of
243 Cretaceous rifting in the Sørvestsnaget Basin ~~seems to have~~ climaxed in the
244 Cenomanian-middle Turonian (Breivik et al., 1998), ~~to become~~ succeeded by Late
245 Cretaceous-Palaeocene fast sedimentation (Ryseth et al., 2003). Particularly the
246 later stages of the basin ~~formation~~ development were strongly influenced by the
247 opening of the North Atlantic (Hanisch, 1984; Brekke & Riis, 1987). Salt diapirism
248 ~~did also contribute~~ to ~~the development~~ structuring of this basin (Perez-Garcia et
249 al., 2013).

250

251 **The Senja Ridge** (SR in Figure 1B) runs parallel to the continental margin and
252 coincides with the western border of the Tromsø Basin. It is characterized by a N-
253 S-trending gravity anomaly which are interpreted as buried mafic-ultramafic
254 intrusions which are associated with the Seiland Igneous Province (Fichler &
255 Pastore 2022). The structural development of the Senja Ridge has been associated
256 with shear affiliated with the development of the shear margin (Riis et al. 1986).
257 ~~and though it was a positive structural element from the mid Cretaceous to the~~
258 ~~Pliocene it may have been activated at an even earlier stage (Gabrielsen et al.~~
259 ~~1990). (Riis et al. 1986).~~

260

261 **The Senja Shear Margin** was active during the Eocene opening of the Norwegian-
262 Greenland Sea during dextral shear that ~~was accompanied~~ splitting out slivers of
263 continental crust. ~~These slivers that~~ became ~~isolated units~~ embedded in the by
264 oceanic crust during continued seafloor spreading (Faleide et al., 2008). The Senja

Formatted: Font: Not Bold

Formatted: Font: Not Bold

265 Shear Margin coincides with the western margin of a basin system [superimposed](#)
266 [on an area of that is characterized by](#) significant crustal thinning. [This part of the](#)
267 [shear margin was characterized by a composite architecture even at the earliest](#)
268 [stages of its development \(Faleide et al., 2008\). The basin system accumulated](#)
269 [sedimentary thicknesses in places exceeding 15 km. The basin system](#)
270 [accumulated and sedimentary thicknesses of up to 18-20km. This part of the shear](#)
271 [margin was characterized by a composite architecture even at the earliest stages](#)
272 [of its development \(Faleide et al., 2008\).](#) Subsequent shearing contributed to the
273 development of releasing and restraining bends, associated pull-apart-basins,
274 neutral strike-slip segments, flower-structures and fold-systems (*sensu* Crowell,
275 1974 a,b; Biddle & Christie-Blick, 1985a,b; Cunningham & Mann, 2007a,b).
276 Particularly the hanging wall west of the Knølegga Fault Complex (see below) of
277 the Barents Shear Margin was affected by wrench deformation as seen from
278 several push-ups and fold systems (Grogan et al., 1999; Bergh & Grogan 2003).
279 The structural development of the margin was complicated by active halokinesis
280 (Knutsen & Larsen, 1997; Gudlaugsson et al., 1998; Ryseth et al., 2003).

281

282

283

284

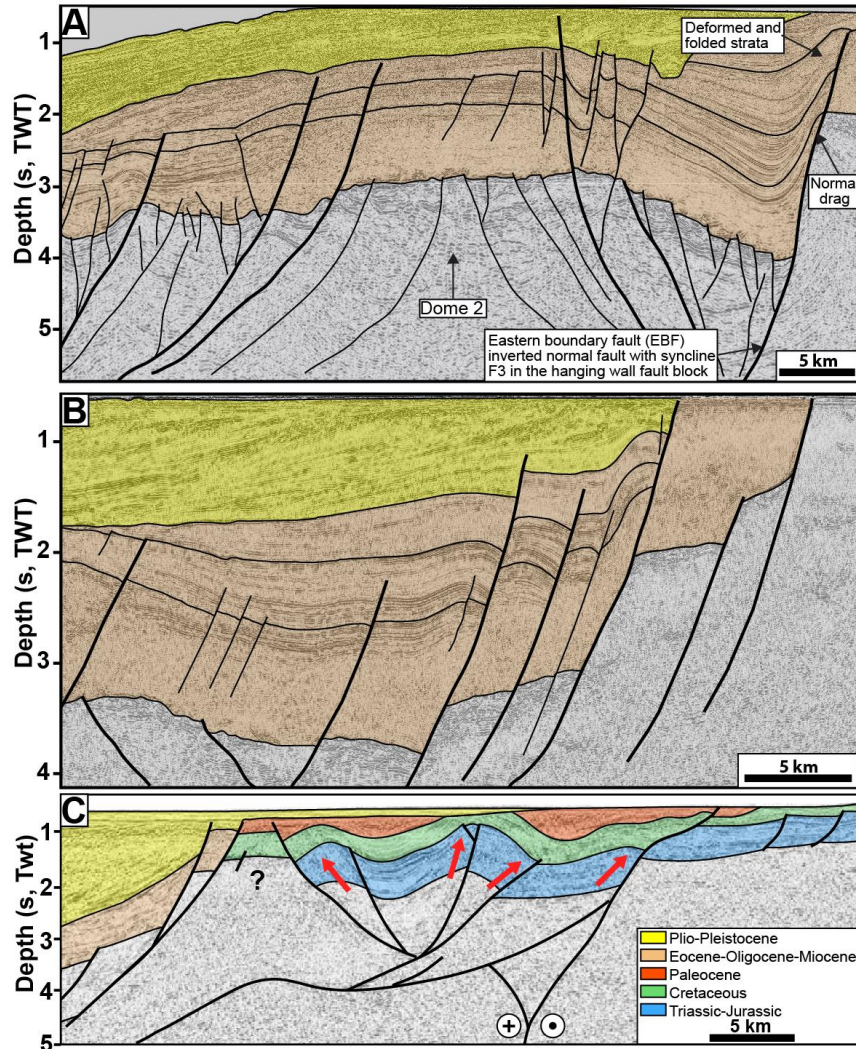
285

286 **Reflection seismic data and structural interpretation**

287 The data set of this study includes 2D seismic reflection data from several surveys and
288 well data in the Vestbakken Volcanic Province. Data coverage is less dense in northern
289 part of the study area. Typical spacing of seismic lines is 4km. Well 7316/5-1 was used
290 to correlate the seismic data with formation tops in the study area whereas published
291 paper based correlations provided calibration and age of each seismic horizon mapped
292 (e.g. Eidvin et al., 1993; 1998 Ryseth et al., 2003). Three stratigraphic groups are
293 present in the well; the Nordland Group (473 - 945 m); the Sotbakken Group (945-
294 3752m) and Nygrunnen Group (3752-4014m) (Eidvin et al., 1993; 1998;
295 www.npd.com). Several folds of regional significance and with axial traces that can be
296 followed along strike for 2-3 km or more occur in the Vestbakken Volcanic Province.
297 The folds commonly are situated in the hanging walls of extensional faults and the fold

298 traces and the structural grain of the thick-skinned master faults are generally parallel.
299 This shows that the position and orientation of the folds were determined by the
300 preexisting structural fabric affiliated with these faults. The continuity of the folds
301 remains obscure due to spacing of reflection seismic lines, so each fold may include
302 undetected overlap zones or axial off-sets that have not been detected. The folds were
303 identified on the lower Eocene, Oligocene and lower Miocene levels. All the mapped
304 folds are either positioned in the hanging walls of extensional (sometimes inverted)
305 master faults or are dissected by younger faults with minor throws.

306
307
308
309
310
311



312

313

314

315

316

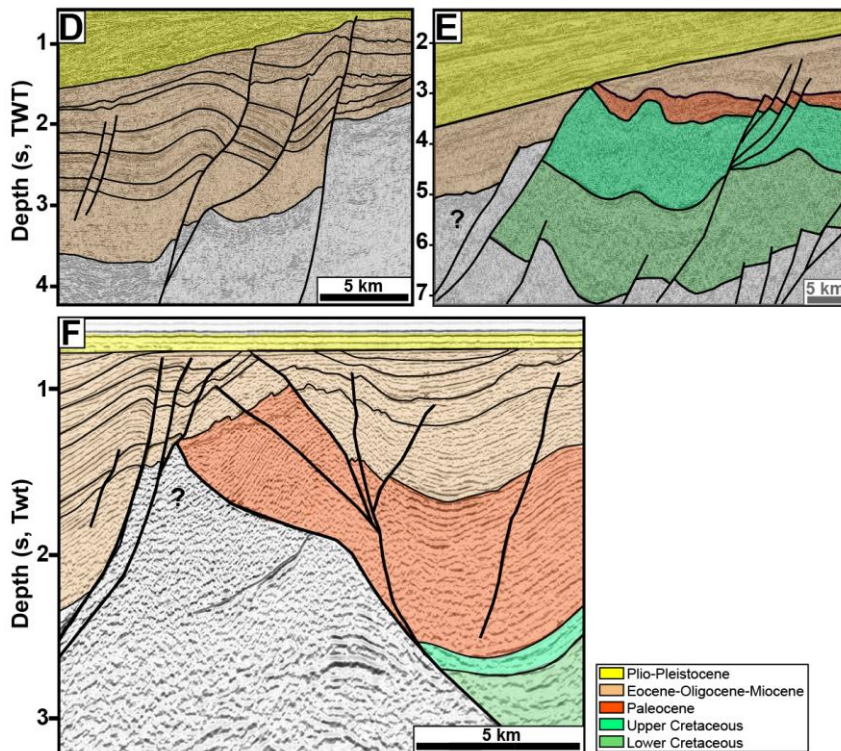
317

318

319

320

321



322

323 **Figure 2:** Seismic examples, Vestbakken Volcanic Province. **A)** Gentle, partly
324 collapsed NE-SW-striking anticline/dome of uncertain origin in the eastern
325 terrace domain of the southern Vestbakken Volcanic Province. **B,C)** Asymmetrical
326 folds (fold family 2; Giannenas 2018) situated along the eastern margin of the
327 Vestbakken Volcanic Province. These may represent primary SPE-4-structures
328 focused in the hanging walls along margins of master fault blocks, representing
329 reactivated SPE-2-structures. **D)** trains of symmetrical folds with upright fold axes
330 (corresponding to PSE-5-structures are preserved inside larger fault blocks. See
331 text for explanation of SPE-structures. **E)** Section through push-up associated with
332 restraining bend (PSE-4-structure). **F)** Flower (PSE-2)-structure in area
333 dominated by neutral shear.
334

335

336 **Strike-slip systems and analogue shear experiments**

337 Shear margins and strike-slip systems are structurally complex and highly
338 dynamic, so that the eventual architecture of such systems include structural
339 elements that were not contemporaneous (e.g. Graymer et al., 2007; Crowell,

340 1962; 1974a,b; Woodcock & Fischer, 1986; Mousloupoulou et al., 2007; 2008).
341 Analogue models offer the option to study the dynamics of such relations and
342 therefore attracted the attention of early workers in this field (eg. Cloos 1928;
343 Riedel 1929) and have continued to do so until today. Early experimental works
344 mostly utilized one-layer (“Riedel-box”) models (e.g. Emmons 1969; Tchalenko,
345 1970; Wilcox et al., 1973), which were soon to be expanded by the study of
346 multilayer systems (e.g. Faugère et al., 1986; Naylor et al., 1986; Richard et al.,
347 1991; Richard & Cobbold, 1989, 1995; Schreurs, 1994, 2003; Manduit & Dauteuil,
348 1996; Dateuil & Mart, 1998; Schreurs & Colletta, 1998, 2003; Ueta et al., 2000;
349 Dooley & Schreurs, 2012). The systematics and dynamics of strike-slip systems
350 have been focused upon in a number of summaries like Sylvester (1985; 1988);
351 Biddle & Christie-Blick (1985a,b); Cunningham & Mann (2007); Dooley &
352 Schreurs (2012); Nemcok et al. (2016) and Peacock et al. (2016). Concepts and
353 nomenclature established in these works are used in the following descriptions
354 and analysis. Also, following Christie-Blick & Biddle (1985a,b) and Dooley &
355 Schreurs (2012) we apply the term Principal Deformation Zone (PDZ) for the
356 junction between the movable polythene plates underlying the experiment. The
357 contact between the fixed and movable base defined a non-stationary velocity
358 discontinuity (“VD”; Ballard et al., 1987; Allemand & Brun, 1991; Tron & Brun,
359 1991).

360 Several experimental works have particularly focused on the geometry and
361 development of pull-apart-basins in releasing bend settings (Mann et al., 1983;
362 Faugère et al. 1983; Richard et al. 1995; Dooley & McClay 1997; Basile & Brun
363 1999; Sims et al., 1999; Le Calvez & Vendeville, 2002; Mann, 2007; Mitra & Paul,
364 2011). The pull-apart basin was described by Burchfiel & Stewart (1966) and
365 Crowell (1974a,b) as formed at a releasing bend or at a releasing fault step-over
366 along a strike-slip zone (Biddle & Christie-Blick 1985a,b). This basin type has also
367 been termed “rhomb grabens” (Freund, 1971) and “strike-slip basins” (Mann et
368 al., 1993) and is commonly considered to be synonymous with the extensional
369 strike-slip duplex (Woodcock & Fischer, 1986; Dooley & Schreurs, 2012). In the
370 descriptions of our experiments, we found it convenient to distinguish between
371 extensional strike-slip duplexes in the context of Woodcock & Fischer (1986) and
372 Twiss & Moores, 2007, p. 140-141;) and pull-apart basins (rhomb grabens:

373 Crowell, 1974a,b; Aydin & Nur, 1993) since they reflect slightly different stages in
374 the development in our experiments (see discussion).

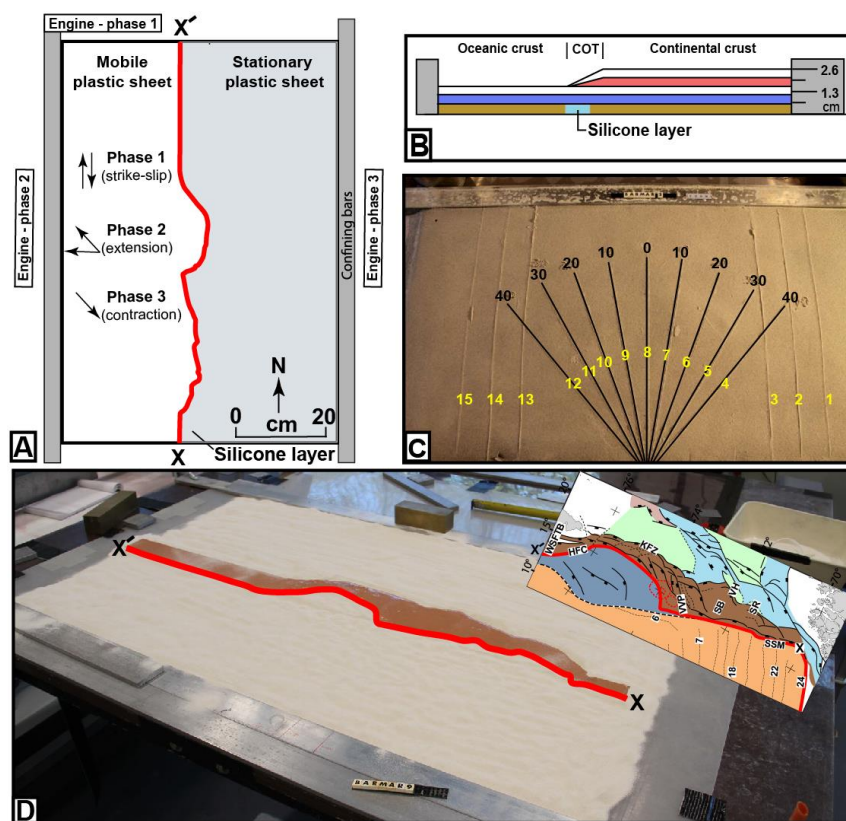
375

376 **Experimental setup**

377 To study the kinematics of complex shear margins, a series of analogue
378 experiments were performed at the tectonic modelling laboratory (TecLab) of
379 Utrecht University, The Netherlands. All experiments were built on two
380 overlapping 1 mm thick plastic sheets (each 100 cm long and 50 cm wide) that
381 were placed on a flat, horizontal table surface. The boundary between the
382 underlying movable and overlying stationary plastic sheets had the shape of the
383 mapped continent-ocean boundary (COB; **Figure 1B**). The moveable sheet was
384 connected to an electronic engine, which pulled the sheet at constant velocity
385 during all three deformation stages. Displacement rates were therefore not scaled.
386 The modelling material was then placed on these sheets where the layers on the
387 stationary sheet represent the continental crust including the continent-ocean
388 transition (COT) whereas those on the mobile sheet represents the oceanic crust.
389 The model layers were confined by aluminum bars along the long sides and sand
390 along the short sides (**Figure 3A**). The continental crust tapers off towards the
391 oceanic crust with a relatively constant gradient. A sand-wedge with a constant
392 dip angle determined by the difference in thickness between the intact and the
393 stretched crust, and that covered the width of the silicon putty layer, was made to
394 simulate the ocean-continent transition (**Figure 3B**). The taper angle was kept
395 constant for all models.

396 The pre-cut shape of the plate boundary includes major releasing bends
397 positioned so that they correspond to the geometry of the COB and the three main
398 structural segments of the Barents Shear Margin as follows. *Segment 1* of the
399 BarMar-experiments (**Figure 4**) contained several sub-segments with releasing
400 and restraining bends as well as segments of “neutral” (Wilcox et al., 1973; Mann
401 et al. 1983; Biddle & Christie-Blick, 1985b) or “pure” (Richard et al., 1991) strike-
402 slip. *Segment 2* had a basic crescent shape, thereby defining a releasing bend at its
403 southern margin in the position similar to that of the Vestbakken Volcanic
404 Province, that merged into a neutral shear-segment along the strike of, whereas a
405 restraining bend occupied the northern margin of the segment. *Segment 3* was a

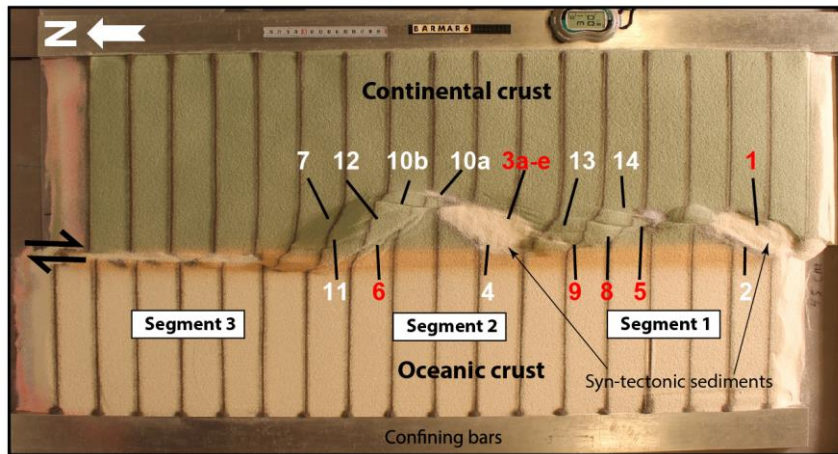
406 straight basement segment, defining a zone of neutral shear and corresponds to
 407 the strike-slip segment west of Svalbard (Figure 1).
 408



409
 410 **Figure 3: A) Schematic set-up of BarMar3-experiment as seen in map view. B)**
 411 **Section through same experiment before deformation, indicating stratification**
 412 **and thickness relations. C) Standard positions and orientation for sections cut in**
 413 **all experiments in the BarMar-series. Yellow numbers are section numbers. Black**
 414 **numbers indicate angle between the margins of the experiment (relative to N-S)**
 415 **for each profile. D) Outline of silicone putty layer as applied in all experiments.**
 416 **Inset shows original structural map of the Barents Margin used to define the width**
 417 **of the thinned crust. Red line (X-X') indicates the western limit of the thinned zone.**
 418

419 The experiments included three stages of deformation with constant rates of
 420 movement of the mobile sheet at 10 cm hr^{-1} in all three stages. The relative angles
 421 of plate movements in the experiments were taken from post late Paleocene
 422 opening directions in the northeast Atlantic (Gaina et al. 2009). Dextral shear was

423 applied in the *first phase* in all experiments by pulling the lower plastic sheet by
424 5cm. In the *second phase* the left side of the experiment was extended by 3 cm
425 orthogonally (BarMar6) or obliquely (31-25 degrees; BarMar 8 & 9) to the trend of



426
427 **Figure 4:** Position of segments and major structural elements as referred to in the
428 text and subsequent figures (see particularly Figures 5 and 6). This example is
429 taken from the reference experiment BarMar6. All experiments BarMar6-9
430 followed the same pattern, and the same nomenclature was used in the
431 description of all experiments and provides the template for the definition of
432 structural elements in Figure 7. Color code for numbers: Red: Faults that were
433 initiated as normal fault. White: faults that were activated as shear faults.
434

435 the shear margin, whereas plate motion was reversed during the *third phase of*
436 *deformation*, leading to inversion of earlier formed basins that had been
437 developed in the strike-slip and extensional phases. Sedimentary basins that
438 develop due to strike-slip (phase 1) or extension (phase 2) have been filled with
439 layers of colored feldspar sand by sieving, so that a smooth surface was obtained.
440 These layers are primarily important for discriminating among deformation
441 phases and thus act as marker horizons. Phase 3 was initiated by inverting the
442 orthogonal (BarMar6) or oblique (BarMar 8 & 9,) extension of Phase 2 to
443 contraction as a proxy for ridge-push that likely was initiated when the mid-
444 oceanic ridge was established in Miocene time in the North Atlantic (Moser et al.,
445 2002; Gaina et al., 2009). Contraction generated by ridge-push has been inferred
446 from the mid Norwegian continental shelf (Våagnes et al., 1998; Pascal & Gabrielsen,
447 2001; Faleide et al., 2008; Gac et al., 2016) and seems still to prevail in the

448 northern areas of Scandinavia (Pascal et al., 2005), although far-field compression
449 generated by other processes have been suggested (eg. Doré & Lundin, 1996). The
450 experiments were terminated before the full closure of the basin system, in
451 accordance with the extension vector > contraction vector as in the North Atlantic
452 (see Vågnes et al. 1998; Pascal & Gabrielsen 2001; Gaina et al. 2009).

453 Coloured layers of dry feldspar sand represent the brittle oceanic and continental
454 crust. This material has proven suitable for simulating brittle deformation
455 conditions (Willingshofer et al., 2005; Luth et al., 2010; Auzemery et al., 2021) and
456 is characterized by a grain size of 100-200µm, a density of 1300 kgm⁻³, a cohesion
457 of ~16-45 Pa and a peak friction coefficient of 0.67 (Willingshofer et al., 2018).
458 Additionally, a 8 mm thick and of variable width corresponding to the transition
459 zone (as mapped in reflection seismic data) of 'Rhodorsil Gomme GSIR' (Sokoutis,
460 1987) silicone putty mixed with fillers was used as a proxy for the thinned and
461 weakened continental crust at the ocean-continent transition (**Figure 1B and**
462 **3A,B**). This Newtonian material (n=1.09) has a density of 1330 kgm⁻³ and a
463 viscosity of 1.42x10⁴ Pa.s.

464 The experiments ~~were have been~~ scaled following standard scaling procedures as
465 described by Hubbert (1937), Ramberg (1967) or Weijermars and Schmeling
466 (1986), assuming that inertia forces are negligible when modelling tectonic
467 processes on geologic timescales (see Ramberg (1981) and Del Ventisette et al.
468 (2007) for a discussion on this topic). The models were scaled so that 10 mm in
469 the model approximates c. 10 km in nature yielding a length scale ratio of 1.00E⁻⁶.
470 As such, the model oceanic and continental crusts scale to 18 and 26 km in nature,
471 respectively, which, although slightly overestimating the most intensely thinned
472 oceanic crust (10-12 km) is in full agreement with the estimated thickness of the
473 thinned oceanward segment of the continental crust (30-20 km Breivik et al.,
474 1998).

475 The brittle crust, dry feldspar sand, deforms according to the Mohr-Coulomb
476 fracture criterion (Horsfield, 1977; Mandl et al., 1977; McClay, 1990; Richard et
477 al., 1991; Klinkmüller et al., 2016), whereas silicone putty promotes ductile
478 deformation and folding. The geometry applied in the present experiments is
479 accordingly well suited for the study of the COB in the Barents Shear Margin
480 (Breivik et al., 1998).

481 When complete, the experiments were covered with a thin layer of sand further to
482 stabilize the surface topography before the models were saturated with water and
483 cross-sections that were oriented transverse to the velocity discontinuity were cut
484 in a fan-shaped pattern (**Figure 3C**). All experiments have been monitored with a
485 digital camera providing top-view images at regular time intervals of one minute.
486

487 All experiments performed were oriented in a N-S-coordinate framework to
488 facilitate comparison with the western Barents Sea area and had a three-stage
489 deformation sequence (dextral shear – [extension](#)~~opening~~ – [contraction](#)~~closure~~). All
490 descriptions and figures relate to this orientation. It was noted that all
491 experiments reproduced comparable basic geometries and structural types,
492 demonstrating robustness against variations in contrasting strength of the
493 “ocean-continent”-transition zone, which included by a zone of silicone putty with
494 variable width below an eastward thickening sand-wedge (**Figure 3B**) and
495 changing displacement velocities. [The experiments were terminated before the
496 full closure of the basin system, in accordance with the extension vector >
497 contraction vector as in the North Atlantic \(see Vågnes et al. 1998; Pascal &
498 Gabrielsen 2001; Gaina et al. 2009\).](#)
499

500 **Modelling Results**

501 A series of nine experiments (BarMar1-9) with the set-up described above was
502 performed. Experiments BarMar1-5 were used to calibrate and optimize
503 geometrical outline, deformation rate, and angles of relative plate movements and
504 are not shown here. The optimized geometries and experimental conditions were
505 utilized for experiments BarMar6-9, of which BarMar6 and 8 (and some examples
506 from BarMar9 and are illustrated here, yielded similar results in that all crucial
507 structural elements (faults and folds) were reproduced in all experiments as
508 described in the text are shown in **Figure 4.**) It is emphasized that the extensional
509 basins affiliated with the extension phase (phase 2) became wider in the
510 orthogonal (BarMar6) as compared to oblique extension experiments (BarMar 8)
511 (**Figures 5 and 6**). Furthermore, the fold systems generated in the experiments
512 that utilized oblique contraction of $31425/13450$ (BarMar8-9) produced more
513 extensive systems of non-cylindrical folds with continuous, but more curved fold

514 traces as compared experiments with orthogonal extension/contraction
515 (BarMar6). The fold axes generally rotated to become parallel to the (extensional)
516 master faults delineating the pull-apart basins generated in deformation stage 1
517 in experiments with an oblique opening/closing angle.

518 Examples of the sequential development is displayed in **Figures 5 and 6**) and
519 summarized in **Figure 7**.

520 Elongated positive structural elements with fold-like morphology as seen on the
521 surface were detected during the various stages of the present experiments. The
522 true nature of those were not easily determined until the experiments were
523 terminated and transects could be examined. Such structures included buried
524 push-ups (*sensu* Dooley & Schreurs, 2012), antiformal stacks, back-thrusts,
525 positive flower structures, fold trains, and simple anticlines. For convenience, we
526 use the non-genetic term “positive structural elements” termed *PSE_{m-n}* for such
527 structure types as seen in the experiments in the following description.

528 In the following the deformation in each segment is characterized for the three
529 deformation phases (**Table 1**).

530
531
532
533

534 **Deformation phase 1: Dextral shear stage**

535

536 *Segment 1*: Differences in the geometry of the pre-cut fault trace between
537 segments 1, 2 and 3 became evident after the very initial deformation stage.
538 Particularly in segments 1 and 3 an array of oblique *en échelon* folds in between
539 Riedel shear structures (*PSE-1-structures*) oriented c. 135°(NW-SE) to the regional
540 VD rotating towards NNW-SSE by continued shear (**Figure 8**; see also Wilcox et
541 al., 1973; Ordonne & Vialon, 1983; Richard et al., 1991; Dooley & Schreurs, 2012).
542 These were simple, harmonic folds with upright axial planes and fold axial traces
543 extending a few cm beyond the surface shear-zone described above. They had
544 amplitudes on the scale of a few millimeters and wavelengths on scale of 5 cm. The
545 *PSE-1-structures* interfered with or were dismembered by younger structures (*Y*-
546 shears and *PSE-2-structures*; see below) causing northerly rotation of individual

547 intra-fault zone lamellae (remnant PSE-1-structures; **Figure 8**). Structures similar
548 to PSE-1-fold arrays are known from almost all strike-slip experiments reported
549 and described in the literature from the early works of (eg. Cloos, 1928; Riedel,
550 1929. See Dooley & Schreurs, 2012 for summary) and are therefore not given
551 further attention here.

552 By 0.25 cm of horizontal displacement in segment 1, which included releasing and
553 restraining bends separated by a central strand of neutral shear, a slightly
554 curvilinear surface trace of a NE-SW-striking, top-NW normal faults in the
555 southernmost part of segment 1 developed. This co-existed with the PSE-1-
556 structures and ~~became~~ ~~was immediately~~ paralleled by a normal fault with
557 opposite ~~dipthrow~~ (fault 2,

558
559
560
561
562

Table 1
 Characteristics of Positive Structural Element (PSE 1-6) as described in the text and shown in figures. Note that the PSE-1-structures that were developed in the earliest stages of the experiments became cannibalized during the continued deformation. No candidates of these structures were identified in the reflection seismic sections..

Struct. type	Structural configuration	Orientation	Expr. stage	Segment	Recognized in seismic	Figure Expr	Figure Seism
PSE-1	Open syn-anticline system	135 deg	Stage 1	1,3	?	5,6	1A?
PSE-2	Incipient flower or half-flower	Parallel master fault	Stage 1	1,2,3	Yes	5,6,8	1B
PSE-3	Forced folds above rotated fault blocks	Parallel master fault in releasing bend	Stage 2	1,2	Yes	9B	
PSE-4	Push-up	Parallel master fault in restraining bend	Stage 1	2	Yes	9D	1C
PSE-5	Anticlines/snake-heads in hanging walls	Parallel master faults	Stage 3	1,2,3	Yes	9C,D	1D,E
PSE-6	Anticline-syncline trains	Parallel master faults	Stage 3	1,2,3	Yes	12	1F

563
564
565
566
567
568

Formatted: Left: 2,54 cm, Right: 2,54 cm, Top: 3,17 cm, Bottom: 3,17 cm, Width: 29,7 cm, Height: 20,99 cm

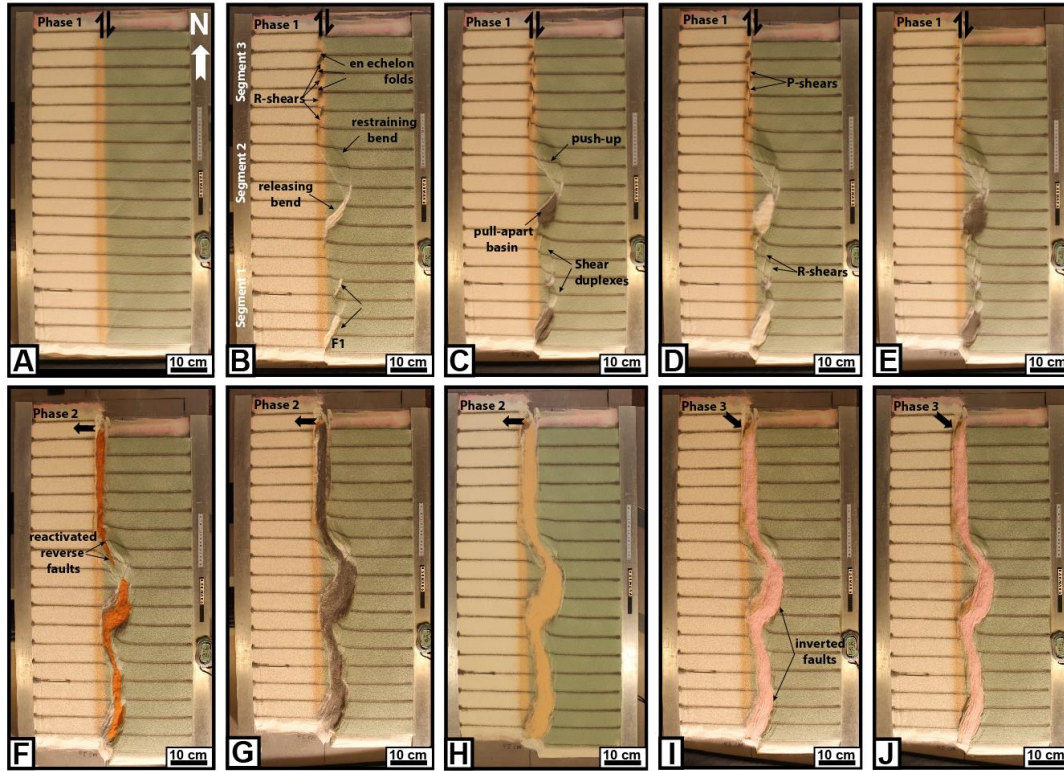
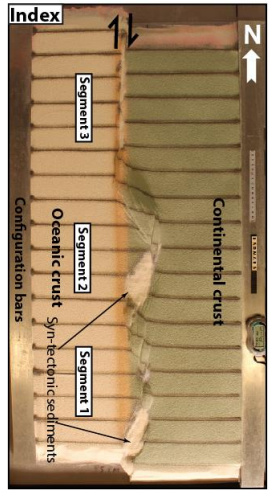
Formatted: English (United States)

Formatted: English (United States)

Formatted: English (United States)

Formatted: English (United States)

Formatted: English (United States)



§70 **Figure 5:** Sequential development of experiment BarMar6 by 0.5, 2.4, 3.5, 4.0 and 5.0 cm of dextral shear (Steps A-E), orthogonal extension
§71 (steps F-H) and oblique contraction (steps I-J). The master fault strands are numbered in **Figure 4**, and the sequential development for
§72 each structural family is shown in **Figure 7**. The reference panel to the ~~upper~~ left shows the positions of the segments.

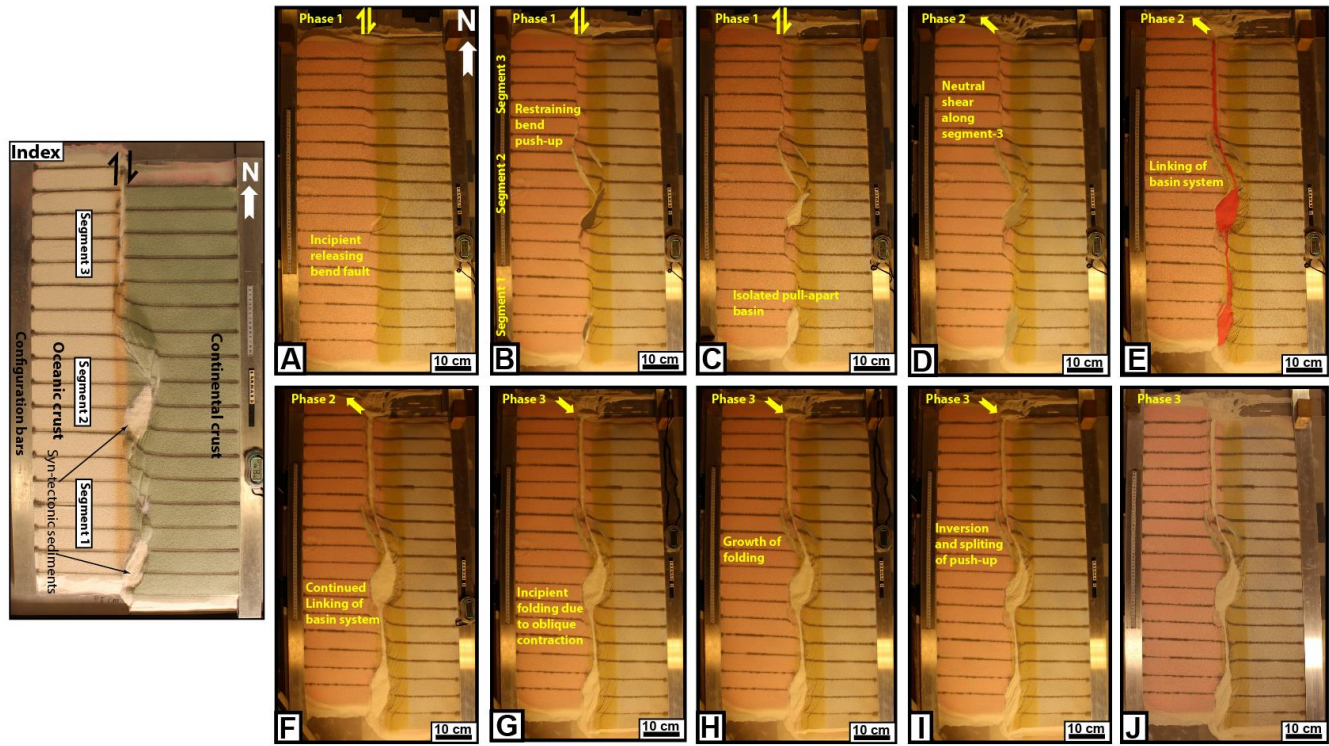
573 **Figure 4)** so that the two faults constrained a crescent- or spindle-shaped
574 incipient extensional shear duplex (**Figures 5B and 6B**; see also Mann et al., 1983;
575 Christie-Blick & Biddle, 1985; Mann 2007; Dooley & Schreurs, 2012).
576 A system of *en échelon* separate N-S to NNE-SSE- striking normal and shear fault
577 segments became visible in segment 1 after ca. 1 cm of shear (**Figure 5C,D**). These
578 faults did not have the orientations as expected for R (Riedel) - and R' (anti-
579 Riedel)- shears (that would be oriented with angles of approximately 15 and 75°
580 from the master fault trace) but became progressively linked ~~withby~~ along strike
581 growth and the development of new faults and fault segments. They thereby
582 acquired the characteristics of Y-shears (oriented sub-parallel to the master fault
583 trace), dissecting the PSE-1-structures. By 2.4 cm of shear, segment 1 had become
584 one unified fault array (**Figure 5D and 6D**), delineating a system of incipient
585 push-ups or positive flower structures (*PSE-2-structures*; **Figures 8 and Figure**
586 **10, sections B1 and B3**); ~~see also; Riedel, 1929; Wilcox et al., 1973; Odonne &~~
587 ~~Vialon, 1983; Dauteuil & Mart, 1995; Dooley & Schreurs, 2012).~~
588 The PSE-2-structures had amplitudes of 1 - 2 cm and wavelengths of 3 - 5 cm as
589 measured on the surface with fault surfaces that steepened down-section, the
590 deepest parts of the structures having cores of sand-layers deformed by open to
591 tight folds. The folds had upright or slightly inclined axial planes, dipping up to
592 55°, mainly to the east. The structures also affected the shallowest layers down to
593 1-2 cm in the sequence, but the shallowest sequences were developed at a later
594 stage of deformation and were characterized by simple gentle to open anticlines.
595 These structures were constrained to a ~~zone of~~ deformation ~~zone~~ directly above
596 the trace of the basement fault, similar to that commonly seen along shear zones
597 (e.g. Tchalenko, 1971; Crowell, 1974 a,b; Dooley & Schreurs, 2012). This zone was
598 3-4 cm wide and remained stable throughout deformation stage 1 and was
599 restricted to the close vicinity of the basement shear fault itself. ~~as also described~~
600 ~~from one-stage shear faults in Riedel box type experiments (e.g. Tchalenko, 1970;~~
601 ~~Naylor et al., 1986; Richard et al., 1991; Casas et al., 2001; Dauteuil & Mart, 1998;~~
602 ~~Dooley & Schreurs, 2012) and from nature as well (e.g. Wilcox et al., 1973;~~
603 ~~Harding, 1974; Harding & Lowell, 1979; Sylvester, 1988; Woodcock & Schubert,~~
604 ~~1994; Mann, 2007).~~

605 -A horse-tail-like fault array developed by ca. 3 cm of shear at the transitions
606 between segments 1 and 2 (~~see also Cunningham & Mann, 2007; Dooley &~~
607 ~~Schreurs, 2012, their Figure 44~~) (**Figures 5B-D and 6B-D**).

608
609 The structuring in *Segment 2*; was ruled by the pre-cut crescent-shaped basement
610 fault (velocity discontinuity~~VD~~) that caused the development of generated -a
611 releasing bend along its southern, and a restraining bend along its northern
612 border (**Figure 11**). The first fault of fault array 3a-e in the southern part of
613 Segment 2 (**Figure 4**) was activated after c. 0.15 cm of bulk horizontal
614 displacement (**Figure 7**). It was

Formatted: Font: Bold

Formatted: Font: Bold



Formatted: Left: 2,54 cm, Right: 2,54 cm, Top: 3,17 cm, Bottom: 3,17 cm, Width: 29,7 cm, Height: 20,99 cm

615
616
617

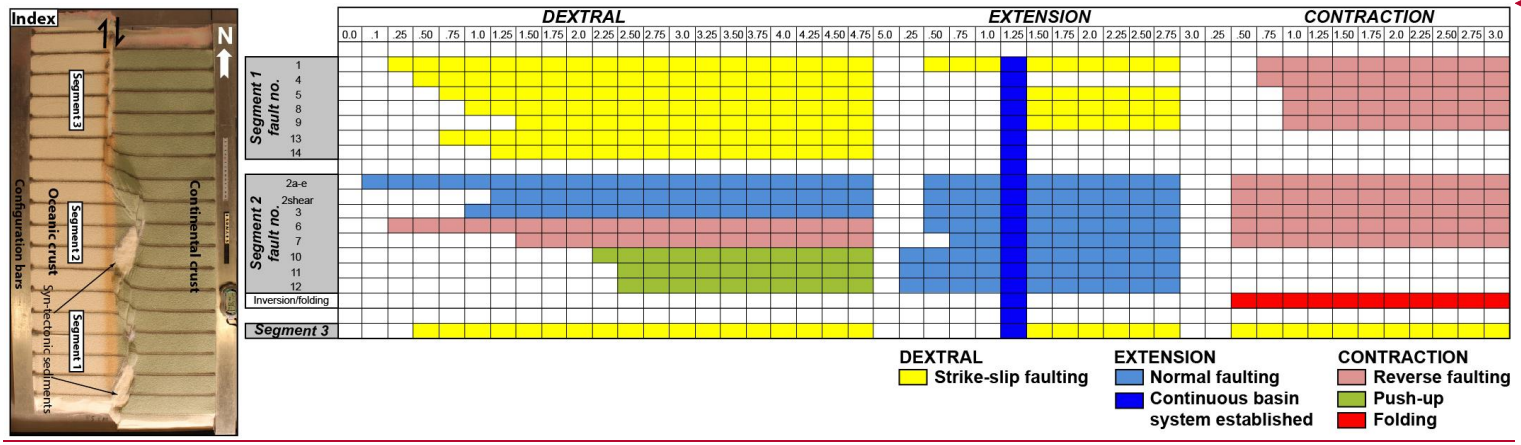
Figure 6: Sequential development of experiment BarMar8 by 0.5, 2.4, 3.5, 4.0 and 5.0 cm of dextral shear (Steps A-E), oblique extension (steps F-H) and oblique contraction (steps I-J). The master fault strands are numbered in **Figure 3**, and the sequential development for

618 each structural family is shown in **Figure 7**. Phases 2 and 3 involved oblique (315°) extension and contraction in this experiment. The
619 reference panel to the ~~upper~~ left shows the positions of the segments.

620 situated directly above the southernmost pre-cut releasing bend, defining the
621 margin of crescent-shaped incipient extensional strike-slip duplexes (in the
622 context of Woodcock & Fischer, 1986, Woodcock & Schubert, 1994 and Twiss &
623 Moores, 2007, p. 140-141). The developing basin got a spindle-shaped structure
624 and developed into a basin with a lazy-S-shape (Cunningham & Mann, 2007; Mann,
625 2007). The basin widened towards the east by stepwise footwall collapse,
626 generating sequentially rotating crescent-shaped extensional fault blocks that
627 became trapped as extensional horses in the footwall of the releasing bend
628 (**Figure 11**). In the areas of the most pronounced extension the crestal part of the
629 rotational fault blocks became elevated above the basin floor, generating ridges
630 that influenced the basin floor topography and hence, the sedimentation. By
631 continued rotation of the fault blocks and simultaneous sieving of sand the crests
632 of the blocks became sequentially uplifted, —generating forced folds (Hamblin,
633 1965; Stearns, 1978; Groshong, 1989; Khalil & McClay, 2016) (**Figure 10A**). In the
634 analysis we used the term *PSE-3-structures* for these features. Simultaneously an
635 expanding sand-sequence became trapped in the footwalls of the master faults,
636 defining typical growth-fault geometries.

637 By a shear displacement of 0.55 cm additional curved splay faults were initiated
638 from the northern tip of the master fault of fault 3f; (**Figure 7**), delineating the
639 northern margin of a rhombohedral pull-apart-basin (Mann et al., 1983; Mann,
640 2007; Christie-Blick & Biddle, 1985) and with a geometry that was
641 indistinguishable from pull-apart basins or rhomb grabens affiliated with
642 unbridged *en échelon* fault arrays (Crowell, 1974 a,b; Aydin & Nur, 1993).
643 Although sand was filled into the subsiding basins to minimize the graben relief
644 and to prevent gravitational collapse, the sub-basins that were initiated in the
645 shear-stage were affected by internal cross-faults, and the initial basin units
646 remained the deepest so that the buried internal basin topography maintained a
647 high relief with several apparent depo-centers separated by intra-basinal
648 platforms.

649 Systems of linked shear faults and PSE-structures became established in the
650 central part with neutral shear that separate the releasing and restraining bends
651 and development similarly to that seen for segment 3 (see below), but these
652 structures were soon destroyed by the combined development of the northern



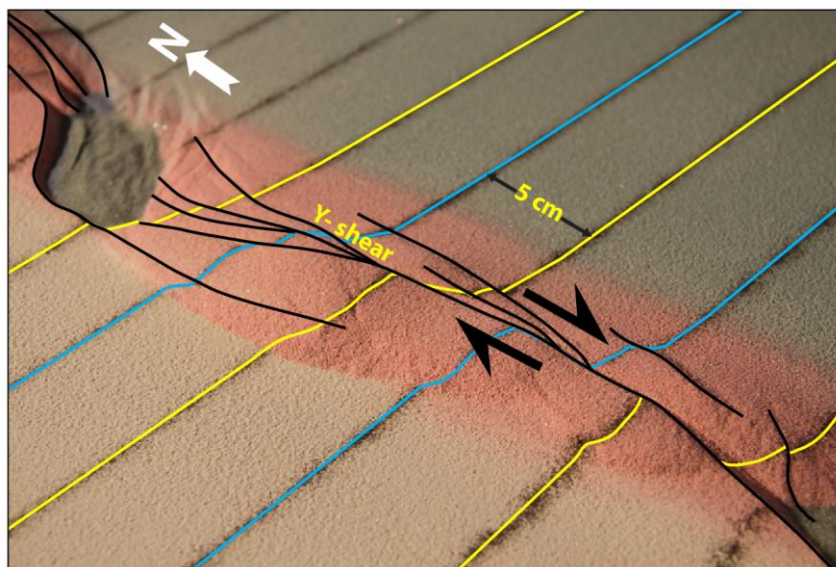
Formatted: Left: 2,54 cm, Right: 2,54 cm, Top: 3,17 cm, Bottom: 3,17 cm, Width: 29,7 cm, Height: 20,99 cm

653
654
655
656
657

Figure 7: Summary of sequential activity in each master fault in Experiment BarMar6 (Figure 5) (for position of each fault, see Figure 4). Type and amount of displacement is shown in two upper horizontal rows. The vertical blue bar indicates the stage at which full along-strike communication became established between marginal basins. Color code (see in-set) indicates type of displacement at any stage. The reference panel to the left shows the positions of the segments.

658 and southern tips of the extensional and contractional shear duplexes (**Figure**
659 **10**).

660 The first structure to develop in the regime of the restraining bend (segment 2;
661 was a top-to-the-southwest (antithetic) thrust fault at an angle of 145° with the
662 regional trend of the basement border as defined by segments 1 and 3 (Fault 6). It
663 became visible by 0.5 cm of displacement. The northern part of segment 2 became,
664 however, dominated by a synthetic contractional top-to-the-northeast fault that
665 was initiated by 0.85 cm of shear (Fault 7 **Figures 5 and 6**). Thus, faults 6 and 7
666 delineated a growing half-crescent-shaped 5-7-cm wide push-up structure (Aydin
667 & Nur, 1982; Mann et al., 1983) south of the restraining bend (**Figure 9**; *PSE-4-*
668 *structures*). By continued shear these structures got the character of an antiformal
669 stack.



670
671 **Figure 8:** PSE-1 anticline-syncline pairs in segment 1 experiment BarMar6 in an
672 oblique view (see Figure 4 for position of Segment 1). PSE-1 folds were
673 constrained to the very fault zone and the fold axes (blue lines) and extended only
674 3-4 cm beyond the fault zone. PSE-2 structures (incipient push-ups and positive
675 flower structures; yellow lines) were delineated by shear faults and completely
676 cannibalized PSE-1 structures by continued shear. Yellow and blue lines show the
677 rotation of the fold axial trace caused by dextral shearing of c. 1.5 cm. 25mm of
678 dextral shear. By a displacement of 35mm the remains of the PSE-1 structure was
679 completely obliterated. The distance between the markers (dark lines) is 5cm.
680 White arrow marks north-direction. Black arrows indicate shear direction.
681

682 *Segment 3* defined a straight strand of neutral shear. Its development in the
683 BarMar-experiments followed strictly that known from numerous published
684 experiments (e.g. Tchalenko, 1970; Wilcox et al., 1973; Harding, 1974; Harding &
685 Lowell, 1979; Naylor et al., 1986; Sylvester, 1988; Richard et al., 1991; Woodcock
686 & Schubert, 1994; Dauteuil & Mart, 1998; Mann, 2007; Casas et al., 2001; Dooley
687 & Schreurs, 2012). A train of Riedel-shears, occupying the full length of the
688 segment, appeared simultaneously on the surface after a shear displacement of
689 0.5 cm, occupying a restricted zone with a width of 2-3 cm. The Riedel-shears
690 dominated the continued structural development of Segment 3. Riedel'-shears
691 were absent throughout the experiments, as should be expected for a sand-
692 dominated sequence (Dooley & Schreurs, 2012). P-shears developed by continued
693 shear, creating linked rhombic structures delineated by the Riedel- and P-shears
694 generating positive structural elements with NW-SE- and NNE-SSE-striking axes
695 (see also Morgenstern & Tchalenko, 1967), soon coalescing to form Y-shears.
696 Transverse sections document that these structures were cored by push-up
697 anticlines, positive half-flower structures and full-fledged positive flower
698 structures in the advanced stages of shear (*PSE-4-structures*) (**Figures 5 and 6.**
699 **See also Figure 10**). These were accompanied by the development of *en échelon*
700 folds and flower structures as commonly reported from strike-slip faults in nature
701 and in experiments. The width of the zone above the basal fault remained almost
702 constant throughout the experiments, but was somewhat wider in experiments
703 with thicker basal silicone polymer layers, similar to that commonly described
704 from comparable experiments (eg. Richard et al., 1991).

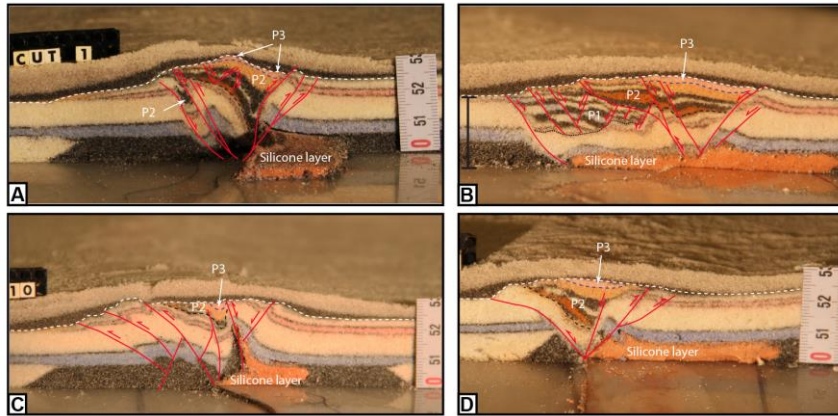
705

706 **Deformation Phase 2: Extension**

707 The late Cretaceous-Palaeocen dextral shear was followed by pure extension
708 accompanying the opening along the Barents Shear Margin in the Oligocene. Our
709 experiments focused on the effects of oblique extension, acknowledging that plate
710 tectonic reconstructions of the North Atlantic suggest an extension angle of $31\pm 25^\circ$
711 ~~as the most likely~~ (Gaina et al., 2009).

712 All strike-slip basins widened in the extensional stage, ~~and most extensively so for~~
713 ~~the experiments with—~~ and as one would expect, the basins generated in
714 orthogonal ~~extension~~ ~~extension~~ became wider than those generated in oblique

715 extension.- In both cases, however, extension promoted The widening of the basin
 716 enhanced the



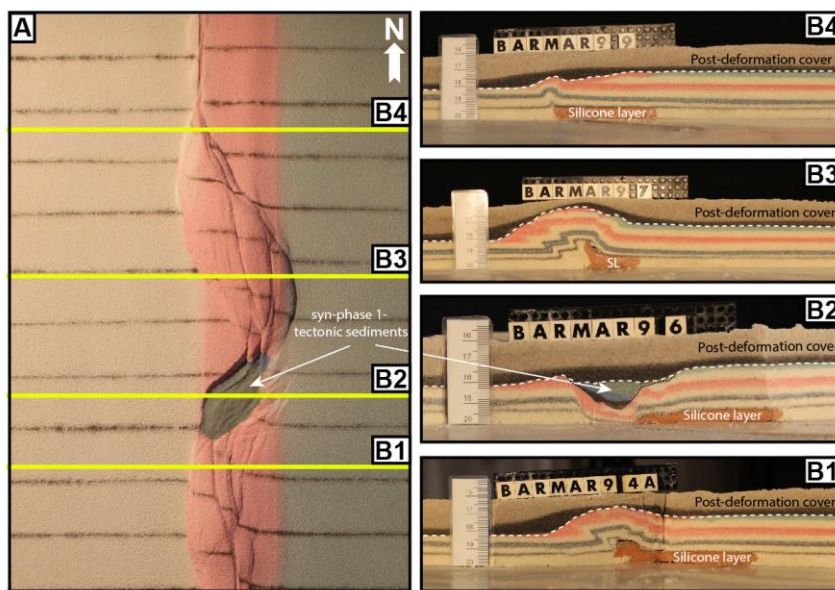
717
 718 **Figure 9:** Cross-sections through PSE-2-related structures. PSE-structures are
 719 marked with P and PSE-number (see also Table 1). **A)** Folded core of incipient
 720 push-up/positive flower structure in segment 1, experiment BarMar6. The fold
 721 structure is completely enveloped of shear faults that have a twisted along-strike
 722 geometry. Note that the eastern margin of the structure developed into a negative
 723 structure at a late stage in the development (filled by black-pink sand sequence)
 724 and that the silicone putty sequence (basal pink sequence) was entirely isolated
 725 in the footwall. **B)** Similar structure in experiment BarMar8. The weak silicone
 726 putty layer here bridged the high-strain zone and focused folding that propagated
 727 into the sand layers (blue). The folds in upper (pink layers) were associated with
 728 the contractional stage, because they contributed to a surface relief filled in by red-
 729 black-sand sequence that was sieved into the margin during the contractional
 730 stage. **C)** Contraction associated with “crocodile structure” in the footwall of the
 731 main fault in segment 1, experiment BarMar8. Note disharmonic folding with
 732 contrasting fold geometries in hanging wall and footwall and at different
 733 stratigraphic levels in the footwall, indicating shifting stress situation in time and
 734 space in the experiment. **D)** Transitional fault strand between to more strongly
 735 sheared fault segments (experiment BarMar9).

737 relief that had been topography already generated in the shear-stage, in the
 738 extensional strike-slip duplex in segment 2 (PSE-3 structures). In the earliest
 739 extensional stage the strike-slip basin in segment 2 dominated the basin
 740 configuration, but by continued extension the linear segments and the minor pull-
 741 apart basins in segments 1 and 2 started to open and to became interlinked,
 742 subsequently generating a linked basin system that runs parallel to ed the entire
 743 shear margin (**Figures 5F-G, 6F-G**). The basins had become completely

744 [interlinked by an extension of 1.25 cm \(marked by the vertical dark blue line in](#)
745 [Figure 7\).](#)

746

747 The orthogonal extension-phase [following dextral strike-slip also](#) reactivated and
748 [very quickly](#) linked several [of the](#) master faults that were established in
749 deformation phase 1 (Figures 5A and 6A). [This became evident already](#) by an
750 extension of 0,25 – 0,50 cm [and](#). [This](#) included the southern fault margin,



751

752 **Figure 10: A)** [contrasting structural styles along the master fault system in](#)
753 [segment 2 in map view and \(B\) cross sections of experiment BarMar9. SL denotes](#)
754 [silicone layer, the stippled line the boundary between pre- and syn-deformation](#)
755 [layers and the white dashed line the boundary with the post-deformation layers.](#)

756

757 the push-up and the splay faults defining [the](#) a crestal collapse graben [of the push-](#)
758 [up](#) (Faults 6, 11 and 12; Figure 4). [All three segments were reactivated in](#)
759 [extension by c. 1.25 cm of orthogonal stretching \(Figure 7\).](#) During the first cm of
760 [extension each basin remained an isolated unit, but after 1 cm of extension all](#)
761 [basins became linked, thus forming one unified elongate extensional basin](#)
762 [\(marked by the vertical dark blue line in Figure 7\) and mainly following the PDZ](#)
763 [as it was cut in the basal templates.](#) Among the faults that [remained](#) were inactive
764 [and remained so](#) throughout the extension phase were the antithetic contractional

765 fault delineating the push-ups in segment 2 ~~towards the south~~ (Fault 6; **Figure 4**).
766 The Y-shear in Segment 3 was reactivated as a straight, continuous extensional
767 fault in ~~phaseStage~~ 2. Total extension in ~~stagePhase 23~~ was 5 cm.

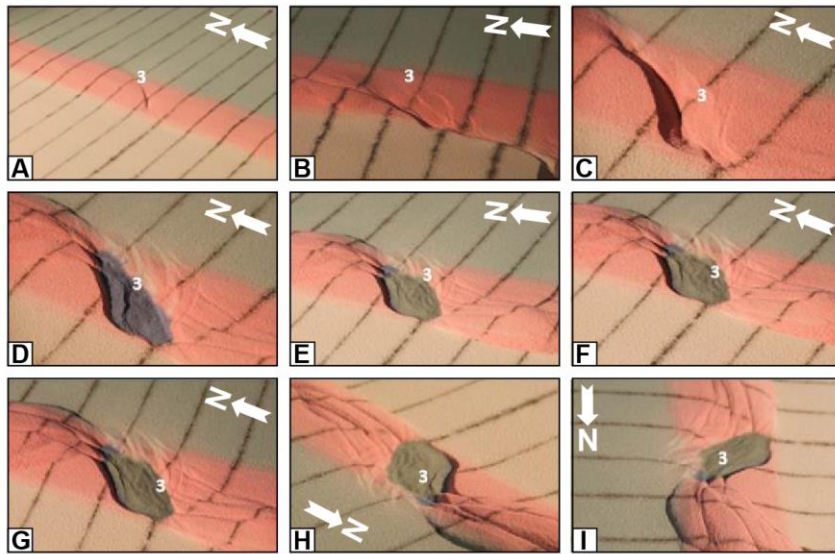
768

769 **Deformation Phase 3: contraction**

770 In our experiments the extension stage was followed by ~~orthogonal or~~ oblique
771 contraction (parallel to the direction of extension as applied for each experiment).

772 ~~The experiments were terminated before the full closure of the basin system, in
773 accordance with the extension vector > contraction vector as in the North Atlantic
774 (see Vågnes et al. 1998; Pascal & Gabrielsen 2001; Gaina et al. 2009).~~

775 A part of the early-stage contraction was accommodated along new faults. It was more
776 common, however, that faults that had been generated in the strike-slip and
777 extensional stages became reactivated and rotated, and the development of
778 isolated folds, which were commonly associated with inverted fault traces,
779 generating snake-head or harpoon-structures structures (Cooper et al., 1989;

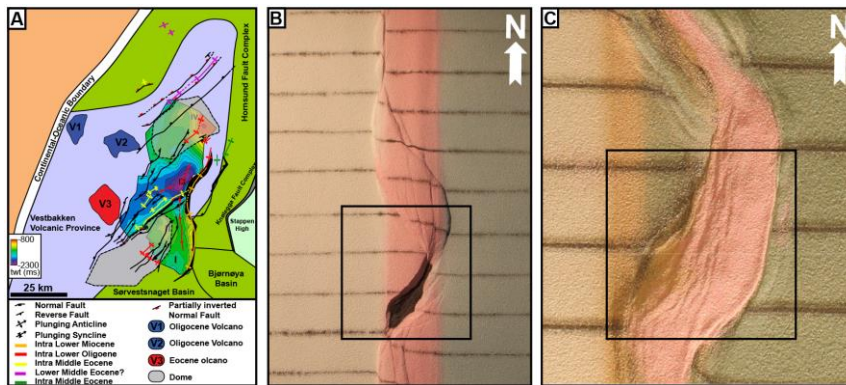


780

781 **Figure 11:** Nine stages in the development of the extensional shear duplex system
782 above the releasing bend in experiment BarMar9. The master faults that
783 developed at an incipient stage (e. Fault 3 that constrained the eastern margin of
784 the extensional shear duplex) remained stable and continued to be active
785 throughout the experiment (Figure 7), but became overstepped by faults in its
786 footwall that became the basin contraction faults at the later stages H and I. The

787 developing basement was stabilized by infilling of gray sand during this part of the
788 experiment. Fault 3 remained active and broke through the basin infill also after
789 the basin infill overstepped the original basin margin. The distance between the
790 markers (dark lines) is 5cm. Yellow arrow marks north-direction. Note that
791 figures “H” and “I” (bottom right) is viewed from directions that differs from the
792 other figures.
793

794 Coward, 1994; Allmendinger, 1998; Yameda & McClay, 2004; Pace & Calamitra,
795 2014); PSE-5-structures). This was particularly the case for the master faults. The
796 dominant structures affiliated with the contractional stage was still new folds with
797 traces oriented orthogonal to the shortening direction and sub-parallel to the
798 preexisting master fault systems that defined the margin and basin margins
799 (**Figure 12**). Also, some deep fold sets that had been generated during the strike-
800 slip phase and seen as domal surface features became reactivated, causing
801 renewed growth of surface structures (see **Figure 10** and explanation in figure
802 caption). These folds were generally up-right cylindrical buckle folds in the initial
803 contractional and with very large trace length: amplitude-ratio (*SPE-6-structures*).
804 Some intra-basin folds, however, defined fold



805
806 **Figure 12: PSE-5-folds generated during phase 3-inversion, experiment BarMar8.**
807 **Note that fold axes mainly parallel the basin rims, but that they deviate from that**
808 **in the central parts of the basins in some cases. The folds are best developed in**
809 **segment 2, which accumulated extension in the combined shear and extension**
810 **stages.**
811

812 arrays that diagonally crossed the basins. Particularly the folds situated along the
813 basin margins developed into fault propagation-folds above low-angle thrust

814 planes. Such faults aligning the western basin margins could have an antithetic
815 attitude relative to the direction of contraction.
816 During the contractional phase the margin-parallel, linked basin system started
817 immediately to narrow and several fault strands became inverted. The basin-
818 closure was a continuous process until the end of the experiment by 3 cm of
819 contraction. The contraction was initiated as a proxy for an ESE-directed ridge-
820 push stage. The first effect of this deformation stage was heralded by uplift of the
821 margin of the established shear zone that that had developed into a rift during
822 deformation stage 2. This was followed by the reactivation and inversion of some
823 master faults (eg. fault a2; eg. **Figure 4**) and thereafter by the development of a
824 new set of low-angle top-to-the-ESE contractional faults. These faults displayed a
825 sequential development, (fault family 1; **Figure 74**) and were associated with
826 folding of the strata in the rift structure, probably reflecting foreland-directed in-
827 sequence thrusting (SPE-5 and PSE-6 fold populations).

828

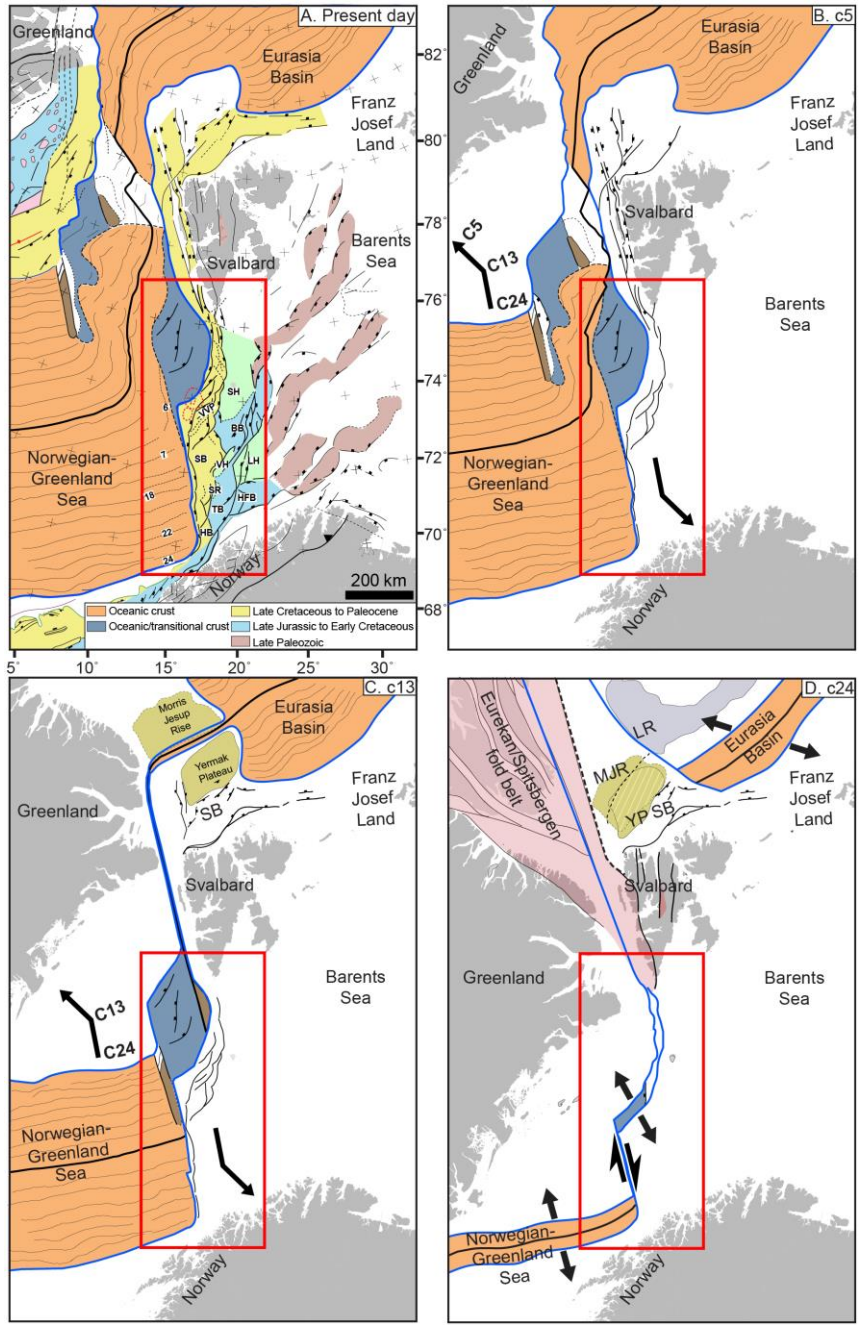
829

830

831 **Discussion**

832 The break-up and subsequent opening of the Norwegian-Greenland Sea was a
833 multi-stage event (**Figure 13**) that imposed shifting stress configurations
834 overprinting the already geometrically complex Barents Shear Margin. Therefore,
835 scaled experiments were designed to illuminate ~~its~~the structural development ~~of~~
836 ~~the Barents Shear Margin~~. The experiments utilized three main segments that
837 correspond to the Senja Fracture Zone (segment 1), the Vestbakken Volcanic
838 Province (segment 2) and the Hornsund Fault Zone (segment 3) respectively and
839 three deformation phases (dextral shear, oblique coextension and contraction).
840 Several~~A series of~~ structural families (PSE 1-6) generated in the experiments
841 correspond to structural features observed in reflection seismic sections.
842 developed during the experiments, most of which correspond to structural
843 elements found along the Barents Shear Margin. In the following discussion we
844 utilize these two data sets in explaining the sequential development of each
845 segment of the shear margin.

§46
§47 Structures of phase 1 (dextral shear)
§48 Segment 1 in the experiments (which corresponds to the Senja Fracture Zone) was
§49 dominated by neutral dextral shear, although subordinate jogs in the (pre-cut)
§50 fault provided minor sub-segments with subordinate releasing and
§51 subordinate restraining bends. PSE-1 folds, that developed at an incipient stage
§52 were immediately paralleled by two sets of normal faults with opposite throw in
§53 the releasing bend areas (eg. fault 2 Figure 4). The two faults defined a crescent-
§54 or spindle-shaped incipient extensional shear duplex (Figures 5B and 6B; see
§55 also Mann et al., 1983; Christie-Blick & Biddle, 1985; Mann, 2007; Dooley &
§56 Schreurs, 2012). The most prominent of these structures corresponds to the
§57 position of the Sørvestsnaget Basin (Figure 1B).
§58 Counterparts to PSE-1 and PSE-2 structural populations observed in the
§59 experiments were not identified with certainty in the seismic data along the
§60 Barents Shear Margin, although some isolated, local anticlinal features could be
§61 dismembered remnants of such. The PSE-1 folds seen in the incipient shear
§62 phase and PSE-2 structures generally belongs to the structural populations that
§63 were developed at the earliest stages of the experiments. Furthermore, these
§64 structure types were confined to the area just above the basal master fault (VD)
§65 and its immediate vicinity (see also experiments in series “e” and “f” of Mitra &
§66 Paul, 2011). Counterparts to PSE-1 structural population were not identified in
§67 the seismic data, although some isolated, local anticlinal features could be
§68 dismembered remnants of such. Because of their constriction to the near vicinity
§69 of the master fault, it is reasonable we speculate that structures generated at an
§70 early stage of shear, are vulnerable to cannibalisation by younger structures with
§71 axes striking parallel to the main shear fault (Y-shears; SPE-2-structures). —We
§72 therefore conclude that the majority of these structure populations were
§73 destroyed during the later stages of shear and during the subsequent stages of
§74 extension and contraction.
§75 PSE-1 folds, that developed at an incipient stage were immediately pursued by the
§76 development of two sets of NNE-SSW-striking normal faults with opposite throws
§77 in the releasing bend areas (eg. fault 2 Figure 4). The two faults defined crescent-
§78 or spindle-shaped incipient extensional shear duplexes. These structures were



879
 880
 881
 882

Figure 13; Main stages in opening of the North Atlantic. The figure builds on figure 5 in Faleide et al. (2008) and has been updated and redrawn.

883
884 stable during the remainder of the experiments and their master faults became
885 reactivated during the extensional and contractional phases (see below). The
886 most prominent of these structures corresponds to the position of the
887 Sørvestsnaget Basin (Figure 1B).
888 During the oblique extension stage segment 1 of experiments BarMar7-9 the basin
889 subsidence was focused in the minor pull-apart basins, which soon became linked
890 along the regional N-S striking basin axis. Remains of several such basin centers,
891 of which the Sørvestsnaget Basin (Knutsen & Larsen, 1997; Kristiansen et al.,
892 2017) is the largest, are preserved and found in seismic data (Figure 1b). During
893 the experiments a continuous basin system was developed in the hangingwall side
894 of the master fault, but it is not likely that opening occurred prior to the extension
895 of the margin underlain by continental crust reached a stage where the separate
896 basin units paralleling the Barents Shear Margin became linked.
897 In the subsequent inversion stage, fold trains with axial traces parallel (PSE 5-
898 folds) to the basin axis and the master faults characterized segment 1. Remnants
899 of such folds are locally preserved in the thickest sedimentary sequences affiliated
900 with the Senja Shear Margin.
901
902 Segment 2, which was controlled underlain by a pre-cut crescent-shaped
903 discontinuity in the experiments corresponds to the Vestbakken Volcanic
904 Province and the southern extension of the Knølegga Fault Complex of the Barents
905 Shear Margin that is a branch of the southern part of the Hornsund Fault Zone
906 (Figures 1b and 4). The part of the Vestbakken Volcanic Province that was the
907 subject of structural analysis by Giennenas (2018) corresponds to the southern
908 part of segment 2 in the present experiments. It is dominated by interfering NNW-
909 SSE- and NE-SW striking fold- and fault systems in its the central part of the basin,
910 whereas N-S-structures are more common along its eastern margin (Figure 12A)
911 (Jebsen & Faleide, 1998; Giennenas, 2018).
912 Intra-basinal high platforms and other complex internal configurations seen in
913 the BarMar-experiments mainly reflect step-wise collapse of the intrinsic basin
914 that generated rotational fault blocks, the crests of which separated local
915 sediment accumulations. Such structures are common in strike-slip basins (eg.

Formatted: Font: Italic

916 Dooley & McClay, 1997; Dooley & Schreurs, 2012) and are consistent with the
917 ~~structural configuration with~~ intra-basin depo-centers seen within the
918 Vestbakken Volcanic province and ~~also~~ in the Sørvestsnaget Basin as well
919 (Knutsen & Larsen, 1997; Jebsen & Faleide, 1998; **Figure 13**). The crests of the
920 rotating fault blocks are termed PSE-3-structures above, and such eroded fault
921 block crests are defining the footwalls of major faults in the Vestbakken Volcanic
922 Province, providing space for sediment accumulation in the footwalls. The area
923 that was affected by the basin formation in the extensional shear duplex stage
924 seems to have remained the deepest part of the Vestbakken Volcanic Province,
925 whereas the part formed in basin widening by sequential footwall collapse created
926 a shallower sub-platform (*sensu* Gabrielsen, 1986) (**Figure 11**).
927 The Knølegga Fault Complex occupies a km-wide zone in segment 2. The master
928 fault strand is paralleled by faults with significant normal throws on its hanging
929 wall side and this belongs to the larger Knølegga Fault Complex (EBF; Eastern
930 Boundary Fault; Giannenas, 2018; **Figure 12A**). The EBF zone is a top-west
931 normal fault with maximum throw of nearly 2000 m (3000 meters). It can be
932 followed along its strike for more than 60 km and seems to die out by horse-tailing
933 at its tip-points. The vicinity of the master faults of the Knølegga Fault Complex
934 locally display isolated elongate positive structures constrained by steeply
935 dipping faults. These structures sometimes display internal reflection patterns
936 that seem exotic in comparison to the surrounding sequences. Some of these
937 structures resemble positive flower structures or push-ups or define narrow
938 anticlines. They are found in both the footwall and hanging wall of the border
939 faults and strike parallel to those and the axes of these structures parallel the
940 master faults. The traces of such structures can be followed over shorter distances
941 than the master faults, and do not occur in the central parts of the Vestbakken
942 Volcanic Province. We suggest that the composite geometry of the Knølegga Fault
943 Complex is due to the development of PSE-2-structures within the realm of a pre-
944 existing normal fault zone.
945 Due to the right-stepping geometry during dextral shear in segment 2, the
946 southern and northern parts were in the releasing and restraining bend positions,
947 respectively (eg. Christie-Blick & Biddle, 1985). Hence, the southern part of
948 segment 2 was subject to oblique extension, subsidence and basin formation when

949 [the northern part was subject to oblique contraction, shortening and uplift. The](#)
950 [southern segment expanded to the east and northeast by footwall collapse and](#)
951 [activation of rotating fault blocks that contributed to a basin floor topography that](#)
952 [affected the pattern of sediment accumulation \(Figure 9A, B\).](#)

953
954 The positive structural elements that prevail in *segment 3* belong to the PSE-2-
955 structre population. The structures affiliated with segment 3 in the BarMar-
956 experiments are similar to those seen in the reflection seismic sections along parts
957 of the Spitsbergen and the Senja shear margins (Myhre, et al. 1982) [and elsewhere.](#)
958 ~~Thus, the structuring in the segment 3 in the BarMar experiments display a~~
959 ~~configuration typical for neutral shear~~ (Cloos, 1928; Riedel, 1929; Tchalenko,
960 1970; Wilcox et al., 1973). [In the experiments](#) *én echelon* folds (corresponding to
961 PSE-1-structueres) first became visible, to be succeeded by the development of
962 Riedel- and P-shears (R'-shears were subdued as expected for sand-dominated
963 sequences (Dooley & Schreurs, 2012). Continued shear followed by collapse and
964 interaction between Riedel and P-shears and the subsequent development of Y-
965 shears initiated push-up- and flower-structure with N-S-axes (PSE-2) structures
966 that were expressed as non-cylindrical (double-plunging) anticlines on the
967 surface (eg. Tchalenko, 1970; Naylor et al., 1986). Structures similar to the PSE-2-
968 structures that were initiated in the present experiments [are common](#) ~~have~~
969 ~~previously been reported from similar experiments with viscous basal layers~~
970 ~~covered by sand (e.g. Richard et al., 1991; Dauteuil & Mart, 1998), in scaled~~
971 ~~experiments illustrating the influence of a~~ [with](#) mechanically stratified sequences
972 ~~where viscous basal strata are covered by sand on fold configurations (e.g. Richard~~
973 ~~et al., 1991; Dauteuil & Mart, 1998).~~

974 ~~The Knølegga Fault Complex occupies a km wide zone. The master fault strand is~~
975 ~~paralleled by faults with significant normal throws on its hanging wall side and~~
976 ~~this is considered to be strands belonging to the larger Knølegga Fault Complex~~
977 ~~(EBF; Eastern Boundary Fault; Giannenas, 2018; Figure 12A). The EBF zone is a~~
978 ~~top west normal fault with maximum throw of nearly 2000 ms (3000 meters). It~~
979 ~~can be followed along its strike for more than 60 km and seems to die out by horse-~~
980 ~~tailing at its tip points. The vicinity of the master faults of the Knølegga Fault~~
981 ~~Complex locally display isolated elongate positive structures constrained by~~

982 steeply dipping faults. These structures sometimes display internal reflection
983 patterns that seem exotic or suspect in comparison to the surrounding sequences.
984 Some of these structures resemble positive flower structures or push ups or
985 define narrow anticlines. They are found in both the footwall and hanging wall of
986 the border faults and strike parallel to those and the axes of these structures
987 parallel the master faults. The traces of such structures can be followed over
988 shorter distances than the master faults, and do not occur in the central parts of
989 the Vestbakken Volcanic Province. We speculate that these are rare fragments of
990 dismembered PSE-1 type structures.

991 Due to the right stepping geometry during dextral shear in segment 2, the
992 southern and northern parts were in the releasing and restraining bend positions,
993 respectively (eg. Christie-Blick & Biddle, 1985). Hence, the southern part of
994 segment 2 was subject to oblique extension, subsidence and basin formation when
995 the northern part was subject to oblique contraction, shortening and uplift. The
996 southern segment expanded to the east and northeast by footwall collapse and
997 activation of rotating fault blocks that contributed to a basin floor topography that
998 affected the pattern of sediment accumulation (Figure 9A, B). The crests of the
999 rotating fault blocks are termed PSE-3 structures above, and such eroded fault
1000 block crests are defining the footwalls of major faults in the Vestbakken Volcanic
1001 Province, providing space for sediment accumulation in the footwalls. The area
1002 that was affected by the basin formation in the extensional shear duplex stage
1003 seems to have remained the deepest part of the Vestbakken Volcanic Province,
1004 whereas the part formed in basin widening by sequential footwall collapse created
1005 a shallower sub platform (*sensu* Gabrielsen, 1986) (Figure 11).

1006 1007 Structures of phase 2 (extension)

1008
1009 It is expected that (regional) basin and (local) fault block subsidence became
1010 accelerated during phase 2 (extension), and more so in the orthogonal extension
1011 experiments (BarMar 6) than in the experiments with oblique extension (BarMar
1012 8), but due to stabilization of basins by infilling of sand, this was not documented.
1013 The widening occurred mainly by fault-controlled collapse of the footwalls, and
1014 dominantly along the master faults that corresponded to the Knølegga Fault

1015 Complex, but also new intra-basin cross-faults that were initiated in the shear
1016 stage (see above) became reactivated, contributing to the complexity of the basin
1017 topography. It is not likely that a stage was reached where all (pull-apart) basin
1018 units along the margin became fully linked, although sedimentary communication
1019 along the margin may have become established.

1020 During the oblique extension stage segment 1 of experiments BarMar7-9 the basin
1021 subsidence was focused in the minor pull-apart basins, which soon became linked
1022 along the regional N-S-striking basin axis. Remains of several such basin centers,
1023 of which the Sørvestsnaget Basin (Knutsen & Larsen, 1997; Kristiansen et al.,
1024 2017) is the largest, are preserved and found in seismic data (Figure 1b). During
1025 the experiments a continuous basin system was developed in the hanging wall
1026 side of the master fault, but it is not likely that opening occurred prior to the
1027 extension of the margin underlain by continental crust reached a stage where the
1028 separate basin units paralleling the Barents Shear Margin became linked.
1029 In the subsequent inversion stage, fold populations(PSE-5-folds) with axial traces
1030 parallel to the basin axis and the master faults characterized segment 1. Remnants
1031 of such folds are locally preserved in the thickest sedimentary sequences affiliated
1032 with the Senja Shear Margin.

1033 1034 -Structures of phase 3 (contraction)

1035
1036 The contraction (phase 3) clearly reactivated normal faults, probably causing
1037 focusing of hanging wall strain and folding, rotation of fault blocks and steepening
1038 of faults. This means that both intra-basinal and marginal faults in the Vestbakken
1039 Volcanic Province can have suffered late steepening. Contraction expressed as fold
1040 systems with fold axes paralleling the basin margins development seems to
1041 correspond very well to the observed structural configuration of the Vestbakken
1042 Volcanic Province. Here pronounced tectonic inversion is focused along the N-S-
1043 striking basin margins and along some NE-SW-striking faults in the central parts
1044 of the basin. Pronounced shortening also occurred inside individual reactivated
1045 fault blocks either by bulging of the entire sedimentary sequence or as trains of
1046 folds (Figure 12B,C).

1047

Formatted: Font color: Auto

1048 [During phase 3 t](#)The restraining bend configuration in the northern part of
1049 segment 2 was characterized by increasing contraction across strike-slip fault
1050 strands that splayed out to the northwest from the central part of segment 2 in an
1051 early stage of dextral shear. This deformation was terminated by the end of phase
1052 1 by stacking of oblique contraction faults (PSE-5 and PSE-6-structures), defining
1053 and antiformal stack-like structure. This type of deformation falls outside the main
1054 area, but to the north this type of oblique shortening during the Eocene (phase 1)
1055 was accommodated by regional-scale strain partitioning (Leever et al., 2011a,b).
1056 The Vestbakken Volcanic Province is characterized by extensive regional
1057 shortening. Onset of this event of inversion/contraction is dated to early Miocene
1058 (Jebsen & Faleide, 1998, Giennenas, 2018) and this deformation included two main
1059 structural fold styles. The first includes upright to steeply inclined closed to open
1060 anticlines that are typically present in the hanging wall of master faults. These folds
1061 typically have wavelengths in the order of 2.5 to 4.5 kilometers, and amplitudes of
1062 several hundred meters. Most commonly they appear with head-on snakehead-
1063 structures and are interpreted as buckle folds, albeit a component shear may occur in
1064 the areas of the most intense deformation, giving a snake-head-type geometry. The
1065 second style includes gentle to open anticline-syncline pairs with upright or steep to
1066 inclined axial planes open anticlines-synclines with wavelengths in the order of 5 to 7
1067 kilometers and amplitudes of several tens of meters to several hundred meters. We
1068 associate those with the PSE-4-type structures as defined in the BarMar-experiments.
1069 These folds are situated in positions where sedimentary sequences have been pushed
1070 against buttresses provided by master faults along the basin margins. The PSE-6 folds
1071 developed as fold trains in the interior basins, where buttressing against larger fault
1072 walls was uncommon. Also, this pattern fits well with the development and geometry
1073 seen in the BarMar-experiments, where folding started in the central parts of the closing
1074 basins before folding of the marginal parts of the basin. In the closing stage the folding
1075 and inversion of master faults remained focused along the basin margins.
1076 The experiments clearly demonstrated that contraction by buckle folding was the
1077 main shortening mechanism of the margin-parallel basin system generated in
1078 phase 2 (orthogonal or oblique extension) in all segments. In the Vestbakken
1079 Volcanic Province segments of the Knølegga Fault Complex, the EBF and the major
1080 intra-basinal faults contain clear evidence for tectonic inversion, whereas this is

1081 less pronounced in others. The hanging wall of the EBF is partly affected by fish-
1082 hook-type inversion anticlines (Ramsey & Huber, 1987; Griera et al., 2018)
1083 (**Figure 2D, E**), or isolated hanging wall anticlines or pairs or trains of synclines
1084 and anticlines (e.g.; Roberts, 1989; Coward et al., 1991; Cartwright, 1989; Mitra,
1085 1993; Uliana et al., 1995; Beauchamp et al. 1996; Gabrielsen et al. 1997; Henk &
1086 Nemcok 2008), the fold style and associated faults probably being influenced by
1087 the orientation and steepness of the pre-inversion fault (Williams et al., 1989;
1088 Cooper et al., 1989; Cooper & Warren, 2010). Some structures of this type can still
1089 be followed for many kilometers having consistent geometry and attitude. These
1090 structures have not been much modified by reactivation and are invariably found
1091 in the proximal parts footwalls of master faults, suggesting that these are
1092 inversion structures correlate to PSE-type 5-structures in the experiments
1093 developed in areas of focused contraction along pre-existing fault scarps during
1094 Oligocene inversion.

1095 Trains of folds with smaller amplitudes and higher frequency are sometimes
1096 found in fault blocks in the central part of the Vestbakken Volcanic Province
1097 (**Figure 12AF**). Although these structures are not dateable my seismic
1098 stratigraphical methods (on-lap configurations etc.) we regard these fold strains
1099 to be correlatable with the tight folds generated in the inversion stage in the
1100 experiments (PSE-6-structures) and that they are contemporaneous with the PSE-
1101 5-structures.

1102 Segment 1 in the experiments, that corresponds to the Senja Shear Margin
1103 segment, displays a structural pattern that is a hybrid between segments 1 and 2:
1104 It contains incipient structural elements that were developed in full in segments 2
1105 and 3, segment 2 being dominated by releasing and restraining bend
1106 configurations and segment 3 dominated by neutral shear. Due to internal
1107 configurations, the three segments were affected to secondary (oblique) opening
1108 and contraction in various fashions. Understanding these differences was much
1109 promoted by the comparison of seismic and model data.

1110
1111 [Some considerations about multiphase deformation in shear margins](#)
1112

Formatted: Not Highlight

1113 The Barents Shear Margin is a challenging target for structural analysis both
1114 because it represents a geometrically complex structural system with a multistage
1115 history, but also because high-quality (3D) reflection seismic data are limited and
1116 many structures and sedimentary systems generated in the earlier
1117 tectonothermal stages have been overprinted and obliterated by younger events.
1118 This makes analogue experiments very useful in the analysis, since they offer a
1119 template for what kind of structural elements can be expected. By constraining the
1120 experimental model according to the outline of the margin geometry and imposing
1121 a dynamic stress model in harmony according to the state-of-the-art knowledge
1122 about the regional tectono-sedimentological development, we were able to
1123 interpret the observations done in reflection seismic data in a new light.

1124
1125 Continental margins are commonly segmented containing primary or secondary
1126 transform elements, and pure strike-slip transforms are relatively rare (eg.
1127 Nemcok et al. 2016). Such margins, however, invariably become affected by
1128 extension following break-up and sometimes contraction due to ridge-push or far-
1129 field stress perhaps related to plate reorganization. The complexity of shear
1130 margins has ignited several conceptual discussions. One such discussion concerns
1131 the presence of zones of weakness prior to break-up (eg. Sibuet & Mascle 1978;
1132 Taylor et al. 2009; Gibson et al. 2013; Basile 2015). In the case of the Barents Shear
1133 Margin the de Geer zone provides such a pre-existing zone of weakness, and this
1134 premise was acknowledged when the scaled model was established. The
1135 relevance of our model is therefore constrained to cases where a crustal-scale
1136 zone of weakness existed before break-up. Furthermore, in cases with pre-
1137 existing zones of weakness, our model demonstrates that the inipient architecture
1138 of the margin is important indeed and the detailed geometry and width of the pre-
1139 existing weak zone must be mapped and included in the model.

Formatted: Subscript

1140
1141
1142

1143 **Summary and conclusions**

1144 ~~The Barents Shear Margin is a challenging target for structural analysis both~~
1145 ~~because it represents a geometrically complex structural system with a multistage~~

1146 ~~history, but also because high quality (3D) reflection seismic data are limited and~~
1147 ~~many structures and sedimentary systems generated in the earlier~~
1148 ~~tectonothermal stages have been overprinted and obliterated by younger events.~~
1149 ~~This makes analogue experiments very useful in the analysis, since they offer a~~
1150 ~~template for what kind of structural elements can be expected. By constraining the~~
1151 ~~experimental model according to the outline of the margin geometry and imposing~~
1152 ~~a dynamic stress model in harmony according to the state of the art knowledge~~
1153 ~~about the regional tectono-sedimentological development, we were able to~~
1154 ~~interpret the observations done in reflection seismic data in a new light.~~

1155

1156 Our observations confirmed that the main segments of the Barents Shear Margin,
1157 albeit undergoing the same regional stress regime, display contrasting structural
1158 configurations

1159

1160 The deformation in segment 2 in the BarMar-experiments, was determined by
1161 releasing and restraining bends in the southern and northern parts, respectively.
1162 Thus, the southern part, corresponding to the Vestbakken Volcanic Province, was
1163 dominated by the development of a regional-scale extensional shear duplex as
1164 defined by Woodcock & Fischer (1983) and Twiss & Moores (2007). By continued
1165 shear the basin developed into a full-fledged pull-apart basin or rhomb graben
1166 (Crowell, 1974; Aydin & Nur, 1982) in which rotating fault blocks were trapped.
1167 The pull-apart-basin became the nucleus for greater basin systems to develop in
1168 the following phase of extension also providing the space for folds to develop in
1169 the contractional phase.

1170

1171 We conclude that fault- and fold systems found in the realm of the Vestbakken
1172 Volcanic Province are in accordance with a three-stage development that includes
1173 dextral shear followed by oblique extension and contraction (3125/1345°) along a
1174 shear margin with composite geometry.

1175 Folds with NE-SW-trending fold axes that are dominant in wider area of the
1176 Vestbakken Volcanic Province and are dominated by folds in the hanging walls of
1177 (older) normal faults, sometimes characterized by narrow, snake-head- or
1178 harpoon-type structures that are typical for tectonic inversion (Cooper et al.,

1179 1989; Coward, 1994; Allmendinger, 1998; Yameda & McClay, 2004; Pace &
1180 Calamitra, 2014) typical of inverted faults.

1181

1182 Comparing seismic mapping and analogue experiments it is evident that a main
1183 challenge in analyzing the structural pattern in shear margins of complex
1184 geometry and multiple reactivation is the low potential for preservation of
1185 structures that were generated in the earliest stages of the development.

1186

1187

1188

1189

1190

1191

1192

1193

1194

1195

1196

1197

1198

1199

1200

1201

1202

1203

1204

1205

1206

1207

1208

1209

1210

1211

1212 **Author contribution**

1213 R.H.Gabrielsen: Contributions to outline, design and performance of experiments.

1214 First writing and revisions of manuscript. First drafts of figures.

1215 P.A.Giennenas: Seismic interpretation in the Vestbakken Volcanic Province.

1216 Identification and description of fold families.

1217 Suggestion:

1218 D.Sokoutis: Main responsibility for set-up, performance and handling of

1219 experiments. Revisions of manuscript.

1220 E.Willigshofer: Performance and handling of experiments. Revisions of

1221 manuscript. Design and revisions of figure material.

1222 M. Hassaan: Background seismic interpretation. Discussions and revisions of

1223 manuscript. Design and revisions of figure material.

1224 J.I.Faleide: Regional interpretations and design of experiments. Participation in

1225 performance and interpretations of experiments. Revisions of manuscript, design

1226 and revisions of figure material.

1227

1228 **Acknowledgements**

1229 The work was supported by ARCEX (Research Centre for Arctic Petroleum

1230 Exploration), which was funded by the Research Council of Norway (grant number

1231 228107) together with 10 academic and six industry (Equinor, Vår Energi, Aker

1232 BP, Lundin Energy Norway, OMV and Wintershall Dea) partners. Muhammad

1233 Hassaan was funded by the Suprabasins project (Research Council of Norway

1234 grant no. 295208). We thank to Schlumberger for providing us with academic

1235 licenses for Petrel software to do seismic interpretation. Two anonymous

1236 reviewers and the editors of this special volume provided comments, suggestions

1237 and advice that enhanced the clarity and scientific quality of the paper.

1238

1239

1240

1241 **References**

- 1242
1243 Allemand P. ~~and~~ Brun J.P.,~~1991~~: Width of continental rifts and rheological layering
1244 of the lithosphere. *Tectonophysics*, 188, 63-69, [1991](#).
- 1245 Allmendinger, R.W.: ~~1998~~: Inverse and forward numerical modeling of threeshear
1246 fault-propagation folds, *Tectonics*, 17(4), 640-656, [1998](#).
- 1247 Auzemery, A., E. Willingshofer, D. Sokoutis, J.P. Brun ~~and~~ ~~S.A.P.L.~~ Cloetingh,
1248 ~~S.A.P.L.~~,~~2021~~: Passive margin inversion controlled by stability of the mantle
1249 lithosphere, *Tectonophysics*, 817, 229042, 1-17,
1250 <https://doi.org/10.1016/j.tecto.2021.229042>, [2021](#).
- 1251 Aydin, A. ~~and~~ Nur, A.:~~1982~~: Evolution of pull-apart basins and their scale
1252 independence. *Tectonics*, 1, 91-105, [1982](#).
- 1253
1254 Ballard J-F., Brun J-P. ~~and~~ Van Ven Driessche J.,~~1987~~: Propagation des
1255 chevauchements au-dessus des zones de décollement: modèles expérimentaux.
1256 *Comptes Rendus de l'Académie des Sciences, Paris*, 11, 305, 1249-1253, [1987](#).
- 1257
1258 Basile, C.: ~~2015~~ Transform continental margins – Part 1: Concepts and models.
1259 *Tectonophysics*, 661, pp.1-10. doi: 10.1016/j.tecto.2015.08.034, [2015](#).
- 1260
1261 Basile, C. ~~and~~ Brun, J.-P.,~~1997~~: Transtensional faulting patterns ranging from pull-
1262 apart basins to transform continental margins: an experimental investigation, *Journal of*
1263 *Structural Geology*, 21, 23-37, [1997](#).
- 1264
1265 Beauchamp, W., Barazangi, M., Demnati, A. ~~and~~ El Alji, M.:~~1996~~: Intracontinental
1266 rifting and inversion: Missouri Basin and Atlas Mountains, Morocco. *American*
1267 *Association of Petroleum Geologists Bulletin*, 80(9), 1455-1482, [1996](#).
- 1268
1269 Bergh, S.G., Braathen, A. ~~and~~ Andresen, A.,~~1997~~: Interaction of basement-involved
1270 and thin-skinned tectonics in the Tertiary fold-and-thrust belt of Central Spitsbergen,
1271 Svalbard. *American Association of Petroleum Geologists Bulletin*, 81(4), 637-
1272 661, [1997](#).
- 1273
1274 Bergh, S.G. ~~and~~ Grogan, P.,~~2003~~: Tertiary structure of the Sørkapp-Hornsund Region,
1275 South Spitsbergen, and implications for the offshore southern extension of the fold-
1276 thrust-belt. *Norwegian Journal of Geology*, 83, 43-60, [2003](#).
- 1277
1278 Biddle, K.T. ~~and~~ Christie-Blick, N., (eds.),~~1985a~~: Strike-Slip Deformation, Basin
1279 Formation, and Sedimentation: Society of Economic Paleontologists and Mineralogists
1280 Special Publication, 37, 386pp, [1985a](#).
- 1281
1282 Biddle, K.T. ~~and~~ Christie-Blick, N.,~~1985b~~: Glossary — Strike-slip deformation,
1283 basin formation, and sedimentation, ~~in~~: Biddle, K.T., and Christie-Blick, N. (eds.):
1284 Strike-Slip Deformation, Basin Formation, and Sedimentation: Society of Economic
1285 Paleontologists and Mineralogists Special Publication, 37, 375-386, [1985b](#).
- 1286
1287 Blaich, O.A., Tsikalas, F. ~~and~~ Faleide, J.I.,~~2017~~: New insights into the tectono-
1288 stratigraphic evolution of the southern Stappen High and the transition to Bjørnøya

1289 Basin, SW Barents Sea, *Marine and Petroleum Geology*, 85, 89-105, doi:
1290 10.1016/j.marpetgeo.2017.04.015, [2017](#).
1291
1292 Breivik, A.J., Faleide, J.I. [and](#) Gudlaugsson, S.T., ~~1998~~: Southwestern Barents Sea
1293 margin: late Mesozoic sedimentary basins and crustal extension, *Tectonophysics*, 293,
1294 21-44, [1998](#).
1295
1296 Breivik, A.J., Mjelde, R., Grogan, P., Shinamura, H., Murai, Y. [and](#) Nishimura, Y.,
1297 ~~2003~~: Crustal structure and transform margin development south of Svalbard based on
1298 ocean bottom seismometer data. *Tectonophysics*, 369, 37-70 [2003](#).
1299
1300 Brekke, H., ~~2000~~: The tectonic evolution of the Norwegian Sea continen- tal margin
1301 with emphasis on the Vøring and Møre basins: Geological Society, London, Special
1302 Publication, 136, 327-378, [2000](#).
1303
1304 Brekke, H. [and](#) Riis, F., ~~1987~~: Mesozoic tectonics and basin evolution of the
1305 Norwegian Shelf between 60°N and 72°N. *Norsk Geologisk Tidsskrift*, 67, 295-322,
1306 [1987](#).
1307
1308 Burchfiel, B.C. [and](#) Stewart, J.H., ~~1966~~: "Pull-apart" origin of the central segment of
1309 Death Valley, California. *Geological Society of America Bulletin*, 77, 439-442, [1966](#).
1310
1311 Campbell, J.D., ~~1958~~: *En échelon* folding, *Economical Geology*, 53(4), 448-472, [1958](#).
1312
1313 Cartwright, J.A., ~~1989~~: The kinematics of inversion in the Danish Central Graben. in:
1314 M.A.Cooper & G.D.Williams (eds.): *Inversion Tectonics*. Geological Society of
1315 London Special Publication, 44, 153-175, [1989](#).
1316
1317 Casas, A.M., Gapals, D., Nalpas, T., Besnard, K. [and](#) Román-Berdiel, T., ~~2001~~:
1318 Analogue models of transpressive systems, *Jornal of Structural Geology*, 23, 733-743,
1319 [2001](#).
1320
1321 Christie-Blick, N. [and](#) Biddle, K.T., ~~1985~~: Deformation and basin formation along
1322 strike-slip faults. in: Biddle, K.T. & Christie-Blick, N. (eds.): *Strike-slip deformation,*
1323 *basin formation and sedimentation*. Society of Economic Mineralogists and
1324 Palaeontologists (Tulsa Oklahoma), Special Publication, 37, 1-34, [1985](#).
1325
1326 Cloos, H., ~~1928~~: Experimenten zur inneren Tectonick, *Zentralblatt für Mineralogie,*
1327 *Geologie und Palaentologie*, 1928B, 609-621, [1928](#).
1328
1329 Cloos, H., ~~1955~~: Experimental analysis of fracture patterns, *Geological Society of*
1330 *America Bulletin*, 66(3), 241-256, [1955](#).
1331
1332 Cooper, M. [and](#) Warren, M.J., ~~2010~~: The geometric characteristics, genesis and
1333 petroleum significance of inversion structures, in Law, R.D., Butler, R.W.H.,
1334 Holdsworth, R.E., Krabbendam, M. & Strachan, R.A. (eds.): *Continental Tectonics and*
1335 *Mountain Building: The Lagacy of Peache and Horne*, Geological Society of London,
1336 Special Publication, 335, 827-846, [2010](#).

Formatted: English (United States)

Formatted: English (United States)

1337 Paor,D., Stoneley,R., Todd,S.P., Turner,J.P. ~~and~~ Ziegler,P.A.,~~1989~~: Inversion
1338 tectonics – a discussion. Geological Society, London, Special Publications, 44, 335-
1339 347, [1989](#).
1340
1341 Coward, ~~M.~~,~~1994~~: Inversion tectonics, in: Hancock,P.L. (ed.): Continental
1342 Deformation, Pergamon Press, 289-304, [1994](#).
1343
1344 Coward, M.P., Gillcrst, R. ~~and~~ Trudgill, B.,~~1991~~: Extensional structures and their
1345 tectonic inversion in the Western Alps, *in*: A.M.Roberts, G.Yielding & B.Freeman
1346 (eds.): The Geometry of Normal Faults. Geological Society of London Special
1347 Publication, 56, 93-112, [1991](#).
1348
1349 Crowell, J.C.,~~1962~~: Displacement along the San Andreas Fault, California, Geological
1350 Society of America Special Papers, 71, 59pp, [1962](#).
1351
1352 Crowell, J.C.,~~1974a~~: Origin of late Cenozoic basins in southern California. in ~~R.H.Dorr,~~
1353 ~~R.H.~~ ~~and~~ ~~R.H.~~Shaver, ~~R.H.~~ (eds.): Modern and ancient geosynclinal sedimentation.
1354 SEPM Special Publication, 19, 292-303, [1974a](#).
1355
1356 Crowell, J.C., 1974b: Implications of crustal stretching and shortening of coastal
1357 Ventura Basin, *in*: Howell,D.G. (ed.): Aspects of the geological history of the
1358 California continental Borderland, American Association of Petroleum Geologists,
1359 Pacific Section,Publication, 24, 365-382, [1974b](#).
1360
1361 Cunningham, W.D. ~~and~~ Mann, P. (eds.); ~~2007a~~: Tectonics of Strike-Slip Restraining
1362 and Releasing Bends, Geological Society London Special Publication, 290, 482pp,
1363 [2007a](#).
1364
1365 Cunningham, W.D. ~~and~~ Mann, P.;~~2007b~~: Tectonics of Strike-Slip Restraining and
1366 Releasing Bends, *in*: Cunningham,W.D. & Mann,P. (eds.), 2007: Tectonics of Strike-
1367 Slip Restraining and Releasing Bends, Geological Society London Special Publication,
1368 290, 1-12, [2007b](#).
1369
1370 Dauteuil, O. ~~and~~ Mart, Y.,~~1998~~: Analogue modeling of faulting pattern, ductile
1371 deformation, and vertical motion in strike-slip fault zones, Tectonics, 17(2), 303-310,
1372 [1998](#).
1373
1374 Del Ventisette, C., Montanari, D., Sani, F., Bonini, M. ~~and~~ Corti, G.,~~2007~~. Reply to
1375 comment by J. Wickham on ‘‘Basin inversion and fault reactivation in laboratory
1376 experiments’’. Journal of Structural Geology 29, 1417–1418, [2007](#).
1377
1378 Dooley, T. ~~and~~ McClay, K.,~~1997~~: Analog modeling of pull-apart basins, American
1379 Association of Petroleum Geologists Bulletin, 81(11), 1804-1826, [1997](#).
1380
1381 Dooley, T.P. ~~and~~ Schreurs, G.,~~2012~~: Analogue modelling of intraplate strike-slip
1382 tectonics: A review and new experimental results, Tectonophysics, 574-575, 1-71,
1383 [2012](#).
1384

Formatted: Font: Italic

Formatted: English (United States)

1385 Doré, A.G. ~~and~~ Lundin, E.R., 1996: Cenozoic compressional structures on the NE
1386 Atlantic margin: nature, origin and potential significance for hydrocarbon exploration.
1387 Petroleum Geosciences, 2, 299-311, 1996.
1388
1389 Doré, A.G., Lundin, E.R., Gibbons, A., Sømme, T.O. ~~and~~ Tøruðbakken, B.O., 2016:
1390 Transform margins of the Arctic: a synthesis and re-evaluation *in*: Nemcok, M.,
1391 Rybár, S., Sinha, S.T., Hermeston, S.A. & Ledvényiová, L. (eds.): Transform Margins:
1392 Development, Control and Petroleum Systems, Geological Society London, Special
1393 Publication, 431, 63-94, 2016.
1394
1395 Doré, A.G., Lundin, E.R., Jensen, L.N., Birkeland, Ø., Eliassen, P.E. ~~and~~ Fichler,
1396 C., 1999: Principal tectonic events in the evolution of the northwest European Atlantic
1397 margin. In: A.J. Fleet & S.A.R. Boldy (eds.): Petroleum Geology of Northwest Europe:
1398 Proceedings of the Fifth Conference (Geological Society of London), 41-61, 1999.
1399
1400 Eidvin, T., Goll, R.M., Grogan, P., Smelror, M. ~~and~~ Ulleberg, K., 1998: The
1401 Pleistocene to Middle Eocene stratigraphy and geological evolution of the western
1402 Barents Sea continental margin at well site 731675-1 (Bjørnøya West area). Norsk
1403 Geologisk Tidsskrift, 78, 99-123 1988.
1404
1405 Eidvin, T., Jansen, E. ~~and~~ Riis, F., 1993: Chronology of Tertiary fan deposits off the
1406 western Barents Sea: Implications for the uplift and erosion history of the Barents Shelf.
1407 Marine Geology, 112, 109-131, 1993.
1408
1409 Eldholm, O., Faleide, J.I. ~~and~~ Myhre, A.M., 1987: Continent-ocean transition at the
1410 western Barents Sea/Svalbard continental margin. Geology, 15, 1118-1122, 1987.
1411
1412 Eldholm, O., Thiede, J., and Taylor, E., 1989: Evolution of the Vøring volcanic margin,
1413 *in*: Eldholm, O., Thiede, J., and Taylor, E., (eds.): Proceedings of the Ocean Drilling
1414 Program, Scientific Results, 104: College Station (Ocean Drilling Program), TX, 1033-
1415 1065, 1989.
1416
1417 Eldholm, O., Tsikalas, F. ~~and~~ Faleide, J.I., 2002: Continental margin off Norway 62-
1418 75°N: Paleogene tectono-magmatic segmentation and sedimentation. Geological
1419 Society of London Special Publication, 197, 39-68, 2002.
1420
1421 Emmons, R.C., 1969: Strike-slip rupture patterns in sand models, Tectonophysics, 7,
1422 71-87, 1969.
1423
1424 Faugère, E., Brun, J.-P. ~~and~~ Van Den Driessche, J., 1986: Bassins asymétriques en
1425 extension pure et en détachements: Modèles expérimentaux, Bulletin Centre Recherche
1426 Exploration et Production Elf Aquitaine, 10(2), 13-21, 1986.
1427
1428 Faleide, J.I., Bjørlykke, K. ~~and~~ Gabrielsen, R.H., 2015: Geology of the Norwegian
1429 Shelf. *in*: Bjørlykke, K.: Petroleum Geoscience: From Sedimentary Environments to
1430 Rock Physics 2nd Edition, Springer-Verlag, Berlin Heidelberg, Chapter 25, 603-637,
1431 2015.
1432
1433 Faleide, J.I., Myhre, A.M. ~~and~~ Eldholm, O., 1988: Early Tertiary volcanism at the
1434 western Barents Sea margin. *in*: A.C. Morton & L.M. Parsons (eds.): Early Tertiary

Formatted: Norwegian (Bokmål)

Formatted: Norwegian (Bokmål)

Formatted: Norwegian (Bokmål)

1435 volcanism and the opening of the NE Atlantic. Geological Society of London Special
1436 Publication, 39, 135-146, [1988](#).-

1437

1438 [Faleide, J.I., Tsikalas, F., Breivik, A.J., Mjelde, R., Ritzmann, O., Engen, Ø., Wilson, J.](#)
1439 [and Eldholm, O., 2008](#): Structure and evolution of the continental margin off Norway
1440 and the Barents Sea. Episodes, 31(1), 82-91, [2008](#).
1441

1442 [Faleide, J.I., Vågnes, E. and Gudlaugsson, S.T., 1993](#): Late Mesozoic - Cenozoic
1443 evolution of the south-western Barents Sea in a regional rift-shear tectonic setting.
1444 Marine and Petroleum Geology, 10, 186-214, [1993](#).
1445

1446 [Fichler, C. and Pastore, Z., 2022](#): Petrology and crystalline crust in the southwestern
1447 Barents Sea inferred from geophysical data. Norwegian Journal of Geology, 102, 41pp,
1448 <https://dx.doi.org/10.17850/njg102-2-2>, [2022](#).
1449

1450 [Freund, R., 1971](#): The Hope Fault, a strike-slip fault in New Zealand, New Zealand
1451 Geological Survey Bulletin, 86, 1-49, [1971](#).-

1452

1453 [Gabrielsen, R.H., 1986](#): Structural elements in graben systems and their influence on
1454 hydrocarbon trap types. in: A.M. Spencer (ed.): Habitat of Hydrocarbons on the
1455 Norwegian Continental Shelf. Norw. Petrol. Soc. (Graham & Trotman), 55 - 60, [1986](#).-

1456

1457 [Gabrielsen, R.H., Færseth, R.B., Jensen, L.N., Kalheim, J.E. and Riis, F., 1990](#):
1458 Structural elements of the Norwegian Continental Shelf. Part I: The Barents Sea
1459 Region. Norwegian Petroleum Directorate, Bulletin, 6, 33pp, [1990](#).-

1460

1461 [Gabrielsen, R.H., Grunnaleite, I. and Rasmussen, E., 1997](#): Cretaceous and Tertiary
1462 inversion in the Bjørnøyrenna Fault Complex, south-western Barents Sea. Marine and
1463 Petroleum Geology, 14, 165-178, [1997](#).-

1464

1465 [Gac, S., Klitzke, P., Minakov, A., Alexander, Faleide, J.I. and Scheck-Wenderoth, M.,](#)
1466 [2016](#): Lithospheric strength and elastic thickness of the Barents Sea and Kara Sea
1467 region, Tectonophysics, 691, 120-132, doi: 10.106/j.tecto.2016.04.028, [2016](#).-

1468

1469 [Gaina, C., Gernigon, L. and Ball, P., 2009](#): Palaeocene – Recent plate boundaries in
1470 the NE Atlantic and the formation of the Jan Mayen microcontinent. Journal of the
1471 Geological Society, London, 166(4), 601-616, [2009](#).-

1472

1473 [Ganerød, M., Smethurst, M.A., Torsvik, T.H., Prestvik, T., Rousse, S., McKenna, C.,](#)
1474 [van Hinsbergen, D.J.J. and Hendriks, W.W.H., 2010](#): The North Atlantic Igneous
1475 Province reconstructed and its relation to the Plume Generation Zone: the Antrim Lava
1476 Group revisited. Geophysical Journal International, 182, 183-202, doi: 10.1111/j.1365-
246X.2010.04620.x, [2010](#).

1477 [Gibson, G.M., Totterdell, J.M., White, N., Mitchell, C.H., Stacey, A.R., M. P. Morse,](#)
1478 [M.P. and A. Whitaker: Preexisting basement structures and its influence on](#)
1479 [continental rifting and fracture development along Australia's southern rifted margin,](#)
1480 [Journal of the Geological Society of London, 170, 365-377, 2013.](#)
1481

1482 [Giannenas, P.A., 2018](#): The Structural development of the Vestbakken Volcanic

Formatted: Norwegian (Bokmål)

Formatted: English (United States)

Formatted: Norwegian (Bokmål)

Formatted: English (United States)

Formatted: English (United States)

Formatted: English (United States)

Formatted: English (United States)

Formatted: Widow/Orphan control, Tab stops: Not at 1,27 cm + 2,54 cm + 3,81 cm + 5,08 cm + 6,35 cm + 7,62 cm + 8,08 cm + 8,89 cm + 10,16 cm + 11,43 cm + 12,7 cm + 13,97 cm + 15,24 cm

Formatted: English (United States)

Formatted: English (United States)

Formatted: English (United States)

Formatted: Font:

Formatted: Font color: Auto

1483 Province, Western Barents Sea. Relation between Faults and Folds, Unpubl. Master
1484 thesis, University of Oslo 2018, 89 pp, [2018](#).

1485

1486 Graymer, R.W., Langenheim, V.E., Simpson, R.W., Jachens, R.C. and Ponce, D.A.,
1487 [2007](#): Relative simple through-going fault planes at large-earthquake depth may be
1488 concealed by surface complexity of strike-slip faults, *in*: Cunningham, W.D. & Mann, P.
1489 (eds.): Tectonics of Strike-Slip Restraining and Releasing Bends, Geological Society
1490 London Special Publication, 290, 189-201, [2007](#).

1491

1492 Griera, A., Gomez.Rivas, E. and Llorens, M.-G., [2018](#): The influence of layer-
1493 interface geometry of single-layer folding, Geological Society of London Special
1494 Publication 487, SP487:4, [2018](#).

1495

1496 Grogan, P., Østvedt-Ghazi, A.-M., Larssen, G.B., Fotland, B., Nyberg, K., Dahlgren,
1497 S. and Eidvin, T., [1999](#): Structural elements and petroleum geology of the Norwegian
1498 sector of the northern Barents sea. *in*: Fleet, A.J. & Boldry, S.A.R. (eds.): Petroleum
1499 Geology of Northwest Europe: Proceedings of the 5th Conference, Geological Society
1500 of London, 247-259, [1999](#).

1501

1502 Groshong, R.H., [1989](#): Half-graben structures: balanced models of extensional fault
1503 bend folds, Geological Society of America Bulletin, 101, 96-195, [1989](#).

1504

1505 Gudlaugsson, S.T. and Faleide, J.I., [1994](#): The continental margin between
1506 Spitsbergen & Bjørnøya, in: O.Eiken (ed.): Seismic Atlas of Western Svalbard, Norsk
1507 Polarinstitutt Meddelelser, 130, 11-13, [1994](#).

1508

1509 Gudlaugsson, S.T., Faleide, J.I., Johansen, S.E. and Breivik, A.J., [1998](#): Late
1510 Palaeozoic structural development of the south-western Barents Sea. Marine and
1511 Petroleum Geology, 15, 73-102, [1998](#).

1512

1513 Hamblin, W.K., [1965](#): Origin of "reverse drag" on the down-thrown side of normal
1514 faults, Geological Society of America Bulletin, 76, 1145-1164, [1965](#).

1515

1516 Hanisch, J., [1984](#): The Cretaceous opening of the Northeast Atlantic. Tectonophysics,
1517 101, 1-23, [1984](#).

1518

1519 Harding, T.P., [1974](#): Petroleum traps associated with wrench faults. American
1520 Association of Petroleum Geologists Bulletin, 58, 1290-1304, [1974](#).

1521

1522 Harding, T.P. and Lowell, J.D., [1979](#): Structural styles, their plate tectonic habitats,
1523 and hydrocarbon traps in petroleum provinces, American Association of Petroleum
1524 Geologists Bulletin, 63, 1016-1058, [1979](#).

1525

1526 Harland, W.B., [1965](#): The tectonic evolution of the Arctic-North Atlantic Region, in:
1527 Taylor, J.H., Rutten, M.G., Hales, A.L., Shackelton, R.M., Nairn, A.E. & Harland, W.B.,
1528 Discussion, A Symposium on Continental Drift, Philosophical Transactions of the
1529 Royal Society of London, Series A, 258, 1088, 59-75, [1965](#).

1530

1531 Harland, W.B., 1969: Contributions of Spitsbergen to understanding of tectonic
1532 evolution of North Atlantic Region, American Association of Petroleum Geologists,
1533 Memoir 12, 817-851, 1969.
1534
1535 Harland, W.B., 1971: Tectonic transpression in Caledonian Spitsbergen, Geological
1536 Magazine, 108, 27-42, 1971.
1537
1538 Henk, A. and Nemcok, M., 2008: Stress and fracture prediction in inverted half-
1539 graben structures. Journal of Structural Geology, 30(1), 81-97, 2008.
1540
1541 Horni, J.Á., Hopper, J.R., Blischke, A., Geisler, W.H., Stewart, M., Mcdermott, K.,
1542 Judge, M., Erlendsson, Ö. and Árting, U.E., 2017: Regional Distribution of
1543 Volcanism within the North Atlantic Igneous Province. The NE Atlantic Region: A
1544 Reappraisal of Crustal Structure, Tectonostratigraphy and Magmatic Evolution.
1545 Geological Society, London, Special Publications, 447, 105-125,
<https://doi.org/10.1144/SP447.18>, 2017.
1546
1547 Horsfield, W.T., 1977: An experimental approach to basement-controlled faulting.
1548 Geologie en Mijbouw, 56(4), 3634-370, 1977.
1549
1550 Hubbert, M.K., 1937: Theory of scale models as applied to the study of geologic
1551 structures, Bulletin Geological Society of America, 48, 1459-1520, 1937.
1552
1553 Jebsen, C. and Faleide, J.I., 1998: Tertiary rifting and magmatism at the western
1554 Barents Sea margin (Vestbakken volcanic province). III international conference on
1555 Arctic margins, ICAM III; abstracts; plenary lectures, talks and posters, 92, 1998.
1556
1557 Khalil, S.M. and McClay, K.R., 2016: 3D geometry and kinematic evolution of
1558 extensional fault-related folds, NW Red Sea, Egypt. in: Childs, C., Holdsworth, R.E.,
1559 Jackson, C.A.L., Manzocchi, T., Walsh, J.J. & Yielding, G. (eds.): The Geometry and
1560 Growth of Normal Faults, Geological Society, London, Special Publication 439,
1561 doi.org/10.1144/SP439.11, 2016.
1562
1563 Klinkmüller, M., Schreurs, G., Rosenau, M. and Kemnitz, H., 2016: Properties of
1564 granular analogue model materials: a community wide survey. Tectonophysics
1565 684, 23-38. <http://dx.doi.org/10.1016/j.tecto.2016.01.017.feb>, 2016.
1566
1567 Knutsen, S.-M. and Larsen, K.I., 1997: The late Mesozoic and Cenozoic evolution of
1568 the Sørvestsnaget Basin: A tectonostratigraphic mirror for regional events along the
1569 Southwestern Barents Sea Margin? Marine and Petroleum Geology, 14(1), 27-54,
1570 1997.
1571
1572 Kristensen, T.B., Rotevatn, A., Marvik, M., Henstra, G.A., Gawthorpe, R.L. and
1573 Ravnås, R., 2017: Structural evolution of sheared basin margins: the role of strain
1574 partitioning. Sørvestsnaget Basin, Norwegian Barents Sea, Basin Research, 2017), 1-
1575 23, doi:10.1111/bre.12235, 2017.
1576
1577 Le Calvez, J.-H. and Vendeville, B.C., 2002: Experimental designs to mode along
1578 strike-slip fault interaction. in: Scellart, W.P. & Passcheir, C. (eds.). Analogue
1579 Modeling of large-scale Tectonic Processes, Journal of Virtual Explorer, 7, 7-23, 2002.

Formatted: English (United States)

Formatted: English (United States)

Formatted: English (United States)

Formatted: Font: 12 pt

Formatted: Font: 12 pt, Superscript

Formatted: English (United States)

1577
1578 Leever, K.A., Gabrielsen, R.H., Sokoutis, D. ~~and~~ Willingshofer, E., ~~2011a~~: The effect
1579 of convergence angle on the kinematic evolution of strain partitioning in transpressional
1580 brittle wedges: insight from analog modeling and high resolution digital image analysis.
1581 Tectonics, 30, TC2013, 1-25, doi: 10.1029/2009TC002649, ~~2011a~~.
1582
1583 Leever, K.A., Gabrielsen, R.H., Faleide, J.I. ~~and~~ Braathen, A., ~~2011b~~: A
1584 transpressional origin for the West Spitsbergen Fold and Thrust Belt - insight from
1585 analog modeling. Tectonics, 30, TC2014, 1- 24, doi: 10.1029/2010TC002753, ~~2011b~~.
1586
1587 Libak, A., Mjelde, R., Keers, H., Faleide, J.I. ~~and~~ Murai, Y., ~~2012~~: An intergrated
1588 geophysical study of Vestbakken Volcanic Province, western Barents Sea continental
1589 margin, and adjacent oceanic crust, Marine Geophysical Research, 33(2), 187-207,
1590 ~~2012~~.
1591
1592 Lorenzo, J.M., ~~1997~~: Sheared continental margins: an overview, Geo-Marine Letters,
1593 17(1), 1-3, ~~1997~~.

1594 Lowell, J.-D., 1972: Spitsbergen Tertiary orogenic belt and the Spitsbergen fracture
1595 zone, Geol. Soc. Am. Bull., 83, 3091–3102, doi:10.1130/0016-
1596 7606(1972)83[3091:STOBAT]2.0.CO;2, ~~1972~~.

1597 Lundin, E.R. ~~and~~ Doré, A.G., ~~1997~~: A tectonic model for the Norwegian passive
1598 margin with implications for the NE Atlantic.: Early Cretaceous to break-up. Journal
1599 of the Geological Society London, 154, 545-550, ~~1997~~.
1600
1601 Lundin, E.R., Doré, A.G., Rønning, K. ~~and~~ Kyrkjebø, R., ~~2013~~: Repeated inversion
1602 in the Late Cretaceous-Cenozoic northern Vøring Basin, offshore Norway, Petroleum
1603 Geoscience, 19(4), 329-341, ~~2013~~.
1604
1605 Luth, S., Willingshofer, E., Sokoutis, D. ~~and~~ Cloetingh, S., ~~2010~~: analogue modelling
1606 of continental collision: Influence of plate coupling on mantle lithosphere subduction,
1607 crustal deformation and surface topography, Tectonophysics, 4184, 87-102, doi:
1608 10.1016/j.tecto2009.08.043, ~~2010~~.

1609 Maher, H. D., Jr., ~~S~~-Bergh, ~~S~~, ~~A~~-Braathen, ~~A~~ and ~~Y~~-Ohta, ~~Y~~, ~~1997~~: Svartfjella,
1610 Eidembukta, and Daudmannsodden lineament: Tertiary orogen-parallel motion in the
1611 crystalline hinterland of Spitsbergen's fold-thrust belt, Tectonics, 16(1), 88–106,
1612 doi:10.1029/96TC02616, ~~1997~~.

1613 Mandl, G., de Jong, L.N.J. ~~and~~ Maltha, A., ~~1977~~: Shear zones in granular material.
1614 Rock Mechanics, 9, 95–144, ~~1977~~.
1615
1616 Manduit, T. ~~and~~ Dauteuil, O., ~~1996~~: Small scale modeling of oceanic transform zones,
1617 Journal of Geophysical Research, 101(B9), 20195-20209, ~~1996~~.
1618
1619 Mann, P., ~~2007~~: Global catalogue, classification and tectonic origins of restraining and
1620 releasing bends on active and ancient strike-slip fault systems. *in*: Cunningham, W.D.
1621 ~~and~~ Mann, P. (eds.), 2007: Tectonics of Strike-Slip Restraining and Releasing Bends,
1622 Geological Society London Special Publication, 290, 13-142, ~~2007~~.

Formatted: English (United States)

Formatted: English (United States)

Formatted: English (United States)

Formatted: English (United States)

Formatted: English (United States)

Formatted: English (United States)

Formatted: English (United States)

Formatted: English (United States)

Formatted: English (United States)

Formatted: Norwegian (Bokmål)

1623
1624 Mann, P., Hempton, M.R., Bradley, D.C. ~~and~~ Burke, K., ~~1983~~: Development of pull-
1625 apart basins. *Journal of Geology*, 91(5), 529-554, [1983](#).
1626
1627 Mascle, J. & Blarez, E., ~~1987~~: Evidence for transform margin evolution from the Ivory
1628 Coast Ghana continental margin, *Nature*, 326, 378-381, [1987](#).
1629
1630 McClay, K.R., 1990: Extensional fault systems in sedimentary basins. A review of
1631 analogue model studies, *Marine and Petroleum Geology*, 7, 206-233, [1990](#).
1632
1633 Mitra, S., ~~1993~~: Geometry and kinematic evolution of inversion structures. *American*
1634 *Association of Petroleum Geologists Bulletin*, 77, 1159-1191, [1993](#).
1635
1636 Mitra, S. ~~and~~ Paul, D., ~~2011~~: Structural geology and evolution of releasing and
1637 constraining bends: Insights from laser-scanned experimental models, *American*
1638 *Association of Petroleum Geologists Bulletin*, 95(7), 1147-1180, [2011](#).
1639
1640 Morgenstern, N.R. ~~and~~ Tchalenko, J.S., ~~1967~~: Microscopic structures in kaolin
1641 subjected to direct shear, *Géotechnique*, 17, 309-328, [1967](#).
1642
1643 Mosar, J., Torsvik, T.H. & the BAT Team, ~~2002~~: Opening of the Norwegian and
1644 Greenland Seas: Plate tectonics in mid Norway since the late Permian. in: E.Eide (ed.):
1645 BATLAS. Mid Norwegian plate reconstruction atlas with global and Atlantic
1646 perspectives. Geological Survey of Norway, 48-59, [2002](#).
1647
1648 Mouslopoulou, V., Nicol, A., Little, T.A. ~~and~~ Walsh, J.J., ~~2007~~: Terminations of
1649 large-strike-slip faults: an alternative model from New Zealand, in: Cunningham, W.D.
1650 ~~and~~ Mann, P. (eds.): *Tectonics of Strike-Slip Restraining and Releasing Bends*,
1651 *Geological Society London Special Publication*, 290, 387- 415, [2007](#).
1652
1653 Mouslopoulou, V., Nicol, A., Walsh, J.J., Beetham, D. ~~and~~ Stagpoole, V., ~~2008~~:
1654 Quaternary temporal stability of a regional strike-slip and rift fault interaction. *Journal*
1655 *of Structural Geology*, 30, 451-463, [2008](#).
1656
1657 Myhre, A.M. ~~and~~ Eldholm, O., ~~1988~~: The western Svalbard margin (74-80°N). *Marine*
1658 *and Petroleum Geology*, 5, 134-156, [1988](#).
1659
1660 Myhre, A.M., Eldholm, O. ~~and~~ Sundvor, E., ~~1982~~: The margin between Senja and
1661 Spitsbergen Fracture Zones: Implications from plate tectonics. *Tectonophysics*, 89, 33-
1662 50, [1982](#).
1663
1664 Naylor, M.A., Mandl, G. ~~and~~ Sijpestijn, C.H.K., ~~1986~~: Fault geometries in basement-
1665 induced wrench faulting under different initial stress states. *Journal of Structural*
1666 *Geology*, 8, 737-752, [1986](#).
1667
1668 Nemcok, M., Rybár, S., Sinha, S.T., Hermeston, S.A. ~~and~~ Ledvényiová, L., ~~2016~~:
1669 Transform margins: development, controls and petroleum systems – an introduction. *in*:
1670 Nemcok, M., Rybár, S., Sinha, S.T., Hermeston, S.A. ~~and~~ Ledvényiová, L. (eds.):
1671 *Transform Margins: Development, Control and Petroleum Systems*, Geological
1672 Society London, Special Publication, 431, 1-38, [2016](#).

1673
1674 Odonne, F. [and](#) Vialon, P., ~~1983~~: Analogue models of folds above a wrench fault,
1675 Tectonophysics, 99,31-46, [1983](#).
1676
1677 Pace, P. [and](#) Calamita, F., ~~2014~~: Push-up inversion structures v. fault-bend
1678 reactivation anticlines along oblique thrust ramps: examples from the Apennines fold-
1679 and-thrust-belt, Italy, Journal Geological Society London, 171, 227-238, [2014](#).
1680
1681 Pascal, C. [and](#) Gabrielsen, R.H., ~~2001~~: Numerical modelling of Cenozoic stress
1682 patterns in the mid Norwegian Margin and the northern North Sea. Tectonics, 20(4),
1683 585-599, [2001](#).
1684
1685 Pascal, C., Roberts, D. [and](#) Gabrielsen, R.H., ~~2005~~: Quantification of neotectonic
1686 stress orientations and magnitudes from field observations in Finnmark, northern
1687 Norway. Journal of Structural Geology, 27, 859-870, [2005](#).
1688
1689 Peacock, D.C.P., Nixon, C.W., Rotevatn, A., Sanderson, D.J. [and](#) Zuluaga, L.F., ~~2016~~:
1690 Glossary of fault and other fracture networks, Journal of Structural Geology, 92,
1691 12-29, doi: 10.1016/j.jgs2016.09.008, [2016](#).
1692
1693 Perez-Garcia, C., Safranova, P.A., Mienert, J., Berndt, C. [and](#) Andreassen, K., ~~2013~~:
1694 Extensional rise and fall of a salt diapir in the Sørvestsnaget Basin, SW Barents Sea.
1695 Marine and Petroleum Geology, 46, 129-134, [2013](#).
1696
1697 Planke, S., Alvestad, E. and Eldholm, O., ~~1999~~: Seismic characteristics of
1698 basaltic extrusive and intrusive rocks: The Leading Edge, 18(3), 342-348. [https://doi-](https://doi.org/ezproxy.uio.no/10.1190/1.1438289)
1699 [org.uzproxy.uio.no/10.1190/1.1438289](https://doi.org/ezproxy.uio.no/10.1190/1.1438289), [1999](#).
1700
1701 Ramberg, H., ~~1967~~: Gravity, deformation and the Earth's crust, Academic Press, New
1702 York, 214pp, [1967](#).
1703
1704 Ramberg, H., ~~1981~~: Gravity, deformation and the Earth's crust, 2nd edition. Academic
1705 Press, New York 452pp, [1981](#).
1706
1707 Ramsay, J.G. [and](#) Huber, M.I., 1987: The techniques of modern structural geology.
1708 Vol. 2: Folds and fractures. Academic Press, London, 309-700, [1987](#).
1709
1710 Reemst, P., Cloetingh, S. [and](#) Fanavoll, S., ~~1994~~: Tectonostratigraphic modelling of
1711 Cenozoic uplift and erosion in the south-western Barents Sea. Marine and Petroleum
1712 Geology, 11, 478-490, [1994](#).
1713
1714 Richard, P.D., Ballard, B., Colletta, B. [and](#) Cobbold, P.R., ~~1989~~: Naissance et
1715 evolution de failles au dessus d'un décrochement de socle: Modélisation experimental
1716 et tomographie, C. R. Acad.Sci. Paris, 308,9, 2111-2118, [1989](#).
1717
1718 Richard, P.D. [and](#) Cobbold, P.R., ~~1989~~: Structures et fleur positives et décrochements
1719 crustaux: mdélisation analogique et interpretation mechanique, C.R.Acad.Sci.Paris,
1720 308, 553-560, [1989](#).
1721

- 1722 Richard, P. ~~and~~ Krantz, R.W., ~~1991~~: Experiments on fault reactivation in strike-slip
 1723 mode, *Tectonophysics*, 188, 117-131, [1991](#).
 1724
- 1725 Richard, P., Mocquet, B. ~~and~~ Cobbold, P.R., 1991: Experiments on simultaneous
 1726 faulting and folding above a basement wrench fault, *Tectonophysics*, 188, 133-141,
 1727 [1991](#).
 1728
- 1729 Riedel, W., ~~1929~~: Zur Mechanik geologischer Brucherscheinungen. *Centralblatt für*
 1730 *Mineralogie, Geologie und Paläontologie*, 1929B, 354-368, [1929](#).
 1731
- 1732 Riis, F., Vollset, J. & Sand, M., ~~1986~~: Tectonic development of the western margin
 1733 of the Barents Sea and adjacent areas. in: M.T. Halbouty (ed.): *Future petroleum*
 1734 *provinces of the World*. American Association of Petroleum Geologists Memoir, 40,
 1735 661-667, [1986](#).
 1736
- 1737 Roberts, D.G., ~~1989~~: Basin inversion in and around the British Isles, in: M.A. Cooper
 1738 & G.D. Williams (eds.): *Inversion Tectonics*. Geological Society of London Special
 1739 Publication, 44, 131-150, [1989](#).
 1740
- 1741 Ryseth, A., Augustson, J.H., Charnock, M., Haugrud, O., Knutsen, S.-M., Midbøe,
 1742 P.S., Opsal, J.G. ~~and~~ Sundsbø, G., ~~2003~~: Cenozoic stratigraphy and evolution of the
 1743 Sørvestsnaget Basin, southwestern Barents Sea. *Norwegian Journal of Geology*, 83,
 1744 107-130, [2003](#).
- 1745 Saunders, A.D., Fitton, J.G., Kerr, A.C., Norry, M.J., and Kent, R.W., ~~1997~~: The North
 1746 Atlantic Igneous Province: Geophysical Monograph 100, American Geophysical
 1747 Union, pp. 45-93, [1997](#).
- 1748 Scheurs, G., ~~1990~~: Experiments on strike-slip faulting and block rotation, *Geology*,
 1749 22, 567-570, [1990](#).
 1750
- 1751 Schreurs, G., ~~2003~~: Fault development and interaction in distributed strike-slip shear
 1752 zones: an experimental approach. in: Storti, F., Holdsworth, R.E. ~~and~~ Salvini, F.
 1753 (eds): *Intraplate Strike-slip Deformation Belts*, Geological Society of London Special
 1754 Publication, 210, 35-82., [2003](#).
 1755
- 1756 Schreurs, G., ~~and~~ Colletta, B., ~~1998~~. Analogue modelling of faulting in zones of
 1757 continental transpression and transtension. in: Holdsworth, R.E., Strachan, R.A.,
 1758 Dewey, J.F. (eds.), *Continental Transpressional and Transtensional Tectonics*,
 1759 Geological Society of London Special Publication, London, 135, 59-79, [1998](#).
 1760
- 1761 Schreurs, G. ~~and~~ Colletta, B., ~~2003~~: Analogue modelling of continental
 1762 transpression and transtension. in: Scellart, W.P. & Passchier, C. (eds.): *Analogue*
 1763 *Modelling of Large-scale Tectonic Processes*. *Journal of the Virtual Explorer*, 7,
 1764 103-114, [2003](#).
 1765
- 1766 Seiler, C., Fletcher, J.M., Quigley, M.C., Gleadow, A.J. ~~and~~ Kohn, B.P., ~~2010~~:
 1767 Neogene structural evolution of the Sierra San Felipe, Baja California: evidence of
 1768 proto-gulf transtension in the Gulf Extensional Province? *Tectonophysics*, 488(1), 87-
 1769 109, [2010](#).

Formatted: English (United States)

Formatted: English (United States)

Formatted: English (United States)

1770
1771 [Sibuet, J.C. and Mascle, J.: Plate kinematic implications of Atlantic equatorial](#)
1772 [fracture zone trends. Journal of Geophysical Research, 85, 3401-3421, 1978.](#)
1773
1774 Sims, D., Ferrill, D.A. [and](#) & Stamatakos, J.A. ~~1999~~: Role of a brittle décollement in
1775 the development of pull-apart basins: experimental results and natural examples.
1776 Journal of Structural Geology, 21, 533-554. [1999.](#)
1777
1778 Sokoutis D. ~~1987.~~: Finite strain effects in experimental mullions. Journal of Structural
1779 Geology, 9, 233-249. [1987.](#)
1780
1781 Stearns, D.W., 1978: Faulting and forced folding in the Rocky Mountains Foreland,
1782 Geological Society of America Memoir, 151, 1-38. [1978.](#)
1783
1784 Sylvester, A.G. (ed); 1985: Wrench Fault Tectonics, Selected papers reprinted from the
1785 AAPG Bulletin and other geological journals, American Association of Petroleum
1786 Geologists Reprint Series 28,3 74pp. [1985.](#)
1787
1788 Sylvester, A.G. ~~1988~~: Strike-slip faults. Geological Society of America Bulletin, 100,
1789 1666-1703. [1988.](#)
1790
1791 [Taylor, B., Goodlife, A. and Martinez, F.: Initiation of transform faults at rifted](#)
1792 [continental margins, Comptes Rendu Geosciences, 341, 428-438, 2009.](#)
1793
1794 Talwani, M. & Eldholm, O. ~~1977~~: Evolution of the Norwegian-Greenland Sea.
1795 Geological Society of America Bulletin, 88, 969-999. [1977.](#)
1796
1797 Tchalenko, J.S. ~~1970~~: Similarities between shear zones of different magnitudes.
1798 Geological Society of America Bulletin, 81, 1625-1640. [1970.](#)
1799
1800 Tron, V. [and](#) Brun J-P. ~~1991~~: Experiments on oblique rifting in brittle-ductile
1801 systems. Tectonophysics, 188(1/2), 71-84. [1991.](#)
1802
1803 Twiss, R.J. [and](#) Moores, E.M. ~~2007~~: Structural Geology, 2nd Edition, W.H. Freeman
1804 & Co., New York, 736pp. [2007.](#)
1805
1806 Ueta, K., Tani, K. [and](#) Kato, T. ~~2000~~: Computerized X-ray tomography analysis of
1807 three-dimensional fault geometries in basement-induced wrench faulting, Engineering
1808 Geology, 56, 197-210. [2000.](#)
1809
1810 Uliana, M.A., Arteaga, M.E., Legarreta, L., Cerdan, J.J. [and](#) Peroni, G.O. ~~1995~~:
1811 Inversion structures and hydrocarbon occurrence in Argentina. *in*: Buchanan, J.G. &
1812 Buchanan, P.G. (eds.): Basin Inversion, Geological Society London Special
1813 Publication, 88, 211-233. [1995.](#)
1814
1815 Vågnes, E., 1997: Uplift at thermo-mechanically coupled ocean-continent transforms:
1816 modeled at the Senja Fracture Zone, southwestern Barents Sea. Geo-Marine Letters,
1817 17, 100-109. [1997.](#)

1815 Våagnes, E., Gabrielsen, R.H. ~~and~~ Haremo, P.,~~1998~~: Late Cretaceous-Cenozoic
1816 intraplate contractional deformation at the Norwegian continental shelf: timing,
1817 magnitude and regional implications. *Tectonophysics*, 300, 29-46, [1998](#).

1818 Weijermars, R. ~~and~~ Schmeling, H.,~~1986~~. Scaling of Newtonian and non-
1819 Newtonian fluid dynamics without inertia for quantitative modelling of rock flow
1820 due to gravity (including the concept of rheological similarity. *Physics of the Earth
1821 and Planetary Interiors*, 43, 316-330, [1986](#).

1822 Wilcox, R.E., Harding, T.P. ~~and~~ Selly, D.R.,~~1973~~: Basic wrench tectonics. *American
1823 Association of Petroleum Geologists Bulletin*, 57, 74-69, [1973](#).

1824
1825 Williams, G.D., Powell, C.M., ~~and~~ Cooper, M.A.,~~1989~~: Geometry and kinematics of
1826 inversion tectonics. in: M.A.Cooper & G.D.Williams (eds.): *Inversion Tectonics*.
1827 Geological Society of London Special Publication, 44, 3-16, [1989](#).

1828
1829 Willingshofer, E., Sokoutis, D. ~~and~~ Burg, J.-P.,~~2005~~: Lithosphere-scale analogue
1830 modelling of collision zones with a pre-existing weak zone, *in*: Gaps, D., Brun, J.P. &
1831 Cobbold, P.R. (eds.): *Deformation Mechanisms, Rheology and Tectonics: from Minerals
1832 to the Lithosphere*, Geological Society London Special Publication, 43, 277-294, [2005](#).

1833
1834 Willingshofer, E., Sokoutis, D., Beekman, F., Schönebeck, F., Warsitzka, J.-M., Michael,
1835 M. ~~and~~ Rosenau, M.,~~2018~~: Ring shear test data of feldspar sand and quartz sand
1836 used in the Tectonic Laboratory (Teclab) at Utrecht University for experimental Earth
1837 Science applications. V. 1. GFZ Data Service. [https://doi.org/10.5880/idgeo.2018.072,](https://doi.org/10.5880/idgeo.2018.072.2018)
1838 [2018](#).

1839
1840 Woodcock, N.H. ~~and~~ Fisher, M.,~~1986~~: Strike-slip duplexes. *Journal of Structural
1841 Geology*, 8(7), 725-735, [1986](#).

1842
1843 Woodcock, N.H. ~~and~~ Schubert, C.,~~1994~~: Continental strike-slip tectonics. in:
1844 P.L.Hancock (ed.): *Continental Deformation* (Pergamon Press), 251-263, [1994](#).

1845
1846 Yamada, Y. ~~and~~ McClay, K.R.,~~2004~~: Analog modeling of inversion thrust structures,
1847 experiments of 3D inversion structures above listric fault systems, in: McClay, K.R.
1848 (ed.): *Thrust Tectonics and Petroleum Systems*, American Association of Petroleum
1849 Geologists Memoir, 82, 276-302, [2004](#).

1850
1851
1852
1853
1854
1855
1856
1857
1858

1859
1860
1861
1862